

Optimal Harvest-Then-Transmit Scheduling for Throughput Maximization in Time-Varying RF Powered Systems

Feng Shan^{ID}, Member, IEEE, Junzhou Luo^{ID}, Senior Member, IEEE, Qiao Jin^{ID}, Liwen Cao^{ID}, Weiwei Wu^{ID}, Member, IEEE, Zhen Ling^{ID}, Member, IEEE, and Fang Dong^{ID}, Member, IEEE

Abstract—Energy harvesting is a promising technique to address the energy hunger problem for thousands of wireless devices. In Radio Frequency (RF) energy harvesting systems, a wireless device first harvests energy and then transmits data with this energy, hence the ‘harvest-then-transmit’ (HTT) principle is widely adopted. We must carefully design the HTT schedule, *i.e.*, schedule the timing between harvesting and transmission, and decide the data transmission power such that the throughput can be maximized with the limited harvested energy. Distinct from existing work, we assume energy harvested from RF sources is time-varying, which is more practical but more difficult to handle. We first discover a surprising result that the optimal transmission power is independent of the transmission time, but solely depends on the RF harvesting power, for a simple case when the energy harvesting is stable. We then obtain an optimal offline HTT-scheduling for the general case that allows the RF harvesting power to vary with time. To the best of our knowledge, it is the first optimal HTT-scheduling algorithm that achieves maximum data throughput for time-varying RF powered systems. Finally, an efficient online heuristic algorithm is designed based on the offline optimality properties. Simulations show that the proposed online algorithm has superior performance, which achieves more than 90% of the offline maximum throughput in most cases.

Index Terms—Wireless communication networks, algorithm design, wireless power transfer, harvest-then-transmit, radio frequency energy harvesting, time-varying wireless power.

I. INTRODUCTION

THE energy hunger problem is one of the major issues for thousands of wireless devices nowadays, such as wireless sensors, Internet of Things devices, and autonomous vehicles,

Manuscript received 8 December 2023; revised 29 April 2024; accepted 20 May 2024. Date of publication 29 August 2024; date of current version 18 October 2024. This work was supported in part by the National Key Research and Development Program of China under Grant 2021YFB2900100; in part by the National Natural Science Foundation of China under Grant 62232004, Grant 62072101, and Grant 62132009; in part by the Natural Science Foundation of Jiangsu Province under Grant BK20230024; in part by Jiangsu Provincial Key Laboratory of Network and Information Security under Grant BM2003201; in part by the Key Laboratory of Computer Network and Information Integration of the Ministry of Education of China under Grant 93K-9; and in part by the Fundamental Research Funds for the Central Universities. (*Corresponding author: Junzhou Luo*.)

The authors are with the School of Computer Science and Engineering, Southeast University, Nanjing, Jiangsu 211189, China (e-mail: shanfeng@seu.edu.cn; jluo@seu.edu.cn; jinqiao@seu.edu.cn; caoliwen@seu.edu.cn; weiweiwu@seu.edu.cn; zhenling@seu.edu.cn; fdong@seu.edu.cn).

Color versions of one or more figures in this article are available at <https://doi.org/10.1109/JSAC.2024.3431569>.

Digital Object Identifier 10.1109/JSAC.2024.3431569

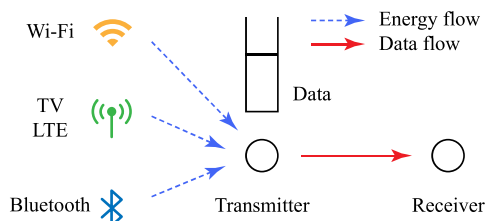


Fig. 1. An illustration of a system that obtains energy from surrounding RF signals and sends its data using the harvested energy.

affecting their working lifetime and thus user experiences. Energy harvesting is a promising technique being developed to address this problem. New research efforts are continuously being made in this direction to harvest energy from various sources. Some recent research work includes magnetic wireless power transfer [1], [2], harvesting energy from the radio frequency [3], [4], solar energy harvesting for electric autonomous vehicles [5], and underwater ultrasonic wireless power transfer [6].

For the vast majority of wireless devices deployed around the human habitat, energy from radio frequency (RF) is one of the important sources. Since the wireless signal not only carries information but also carries power. Hardware for RF power harvesting has been built to harvest energy from everyday radio frequency signals such as TV broadcast signals [7], WiFi signals [8] and Bluetooth signals [9]. Meanwhile, radio wave interference has been utilized to charge multiple devices concurrently [4]. For a long time, off-the-shelf commercial products on RF wireless power transfer (WPT) have been available from both Powercast [10] and WISP [11]. Fig. 1 illustrates such a system that uses harvested energy to power its operations and transmit data.

A wireless device in an RF powered system usually first harvests energy from RF signals and then transmits data with the harvested energy. There are **three primary reasons** that the two operations execute sequentially. *Firstly*, in low-cost sensors, crucial hardware components like antennas are shared by both the harvesting and transmission modules, preventing simultaneous operations [13], [14]. *Secondly*, most energy harvesting devices, including commercial products from Powercast [10] and WISP [11], use supercapacitors as energy buffers, which inherently cannot support concurrent discharging (transmitting data) and recharging (harvesting energy) [12]. *Lastly*, the limited bandwidth needs to be

shared by the two operations. For example, Mohanti et al. [8] propose a time-switching strategy that shares the ISM band for WiFi data transmission and RF WPT; more recently, Clerckx et al. [28] built a practical energy harvesting system that divides operation time into distinct slots for either receiving power or transmitting data.

In this paper, we use ‘harvest-then-transmit’ (HTT) to represent the principle of first harvesting energy then transmission data. HTT schedule has already been widely adopted widely [8], [12], [13], [15], [16], [17], [19], [21], [22].

A. Related Work

Time-varying is one of the most significant features for general energy harvested from the surrounding environment, including energy harvested from RF signal power sources [13], [15], and from other power sources [18]. Despite tremendous research efforts being spent in this direction, how the time-varying RF power affects the wireless data throughput, even for a simple scenario including only one transmitter and one receiver, is not yet fully investigated.

This paper therefore studies such a fundamental HTT scheduling problem aiming at transmitting the maximum data in a given time duration, assuming the wireless harvesting power is time-varying. More specially, we wish to optimally determine for the transmitter when to do energy harvesting (charging), when to do data transmission (sending), and what transmission power to use, in order to maximize data transmission with the limited and dynamic harvested power.

Some of the most relevant research work includes [12], [15], [19], [20]. Ju and Zhang [19] are among the first group of researchers to investigate this problem, although they assume constant harvesting power. For one transmitter one receiver scenario, they have observed an important tradeoff that setting a longer charging time leads to a shorter sending time but at a higher transmission rate since more energy was charged, while setting a shorter charging duration results in a lower transmission rate but a longer sending duration. They have proposed a way of finding the best time allocation to achieve maximum data throughput. Zhao et al. [20] have also studied the same throughput maximization problem and proposed a numerically searching technique to solve it. Zewde and Gursoy [15] extends such results on throughput maximization by further considering statistical QoS constraints. Li et al. [12] study the network utility (or throughput) maximization problem for cooperative networks. Although Zewde and Gursoy [15] and Li et al. [12] target advanced topics, they both provide analysis for the simple scenario with only one transmitter and one receiver and constant RF harvesting power. Assuming constant RF harvesting power simplifies the theoretical analysis of HTT and its schedule. However, how the time-varying RF power affects the data throughput remains a theoretically unsolved challenging problem, even for a simple scenario that includes only one transmitter and one receiver.

Distinct from the above most relevant work [12], [15], [19], [20] that aim at the optimal time allocation between charging and sending, we approach the optimal solution from a quite

different angle *i.e.*, by targeting the optimal data transmission power. This new approach has led us to discover a surprising result. Our previous work [16], [17] assumes the stable power transfer and studies a different optimization problem, *i.e.*, design an HTT schedule to achieve the minimum delay for transmitting a given set of data packets. These previous works of ours have inspired the discovery of the basic results of this paper.

Extensive research efforts have been devoted to various topics in RF powered systems. One of the most notable system-building works comes from Clerckx and his coauthors [28], [29]. The system they developed harvests RF energy from the electromagnetic waves of distributed antennas. More specifically, their system has two antennas: one is dedicated to harvesting energy, and the other is for transmitting data. Meanwhile, time is divided into slots, each slot being assigned either for energy harvesting or data transmission. Alcaraz Lopez et al. [30] surveyed the research area of RF harvesting, categorizing the harvesting methods based on the number of antennas used and how these antennas are organized to harvest RF energy. Both Alcaraz Lopez et al. [31] and Valentini et al. [32] allow energy to accumulate over time beyond a single ‘harvest-and-transmit’ round, while the former focuses on a finite battery and finite block length, and the latter studies the problem when the batteries are affected by aging. Huang et al. [33] studied a more general problem of one-to-many RF power transfer, investigating how to determine the harvest-transmit time ratio and transmission power. Choi et al. [34] allow random access to the wireless broadcast medium. They focus on the harvest-or-access problem for each time slot. Karadag et al. [35] explore how to control power and allocate harvest-transmit time, by proving the NP-hardness and then proposing heuristic algorithms.

The time-varying power harvested from harvesting is one of the most important characteristics and is assumed by some recent research work [18]. Qureshi and Tekin [18] design transmission rate selection online algorithm for cognitive radio networks assuming the dynamic power from an energy harvesting source. Kim et al. [23] provides a power allocation policy based on reinforcement learning, assuming random energy arrival and time-varying channels. Zhang et al. [24] design a general framework to solve the public goods problem for the WPT network, considering the time-varying channel condition.

While general energy harvesting from the surrounding environment has been discussed, RF Wireless Power Transfer (WPT) proves to be a more reliable solution for the vast majority of wireless devices deployed in human habitats.

B. Motivation and Contributions

From the above discussion, we are motivated by the need to design an efficient *HTT-scheduling* to achieve maximum data throughput for time-varying RF powered systems. The motivations for our work are listed below.

- There is a lack of optimal results for this fundamental problem, despite the tremendous research efforts that

have been expended in this direction. Most related work assumes that the wireless power transfer is stable and static. Whether there exists an optimal solution for the fundamental throughput maximization problem for time-varying RF powered systems in a simple scenario with only one transmitter and one receiver is still open.

- We are encouraged by our previous work. Although our previous work [16], [17] studies a different problem and assumes constant energy harvesting from RF power, we do get inspired by handling the tradeoff of charging and sending. We attack the new optimization problem with a quite different approach, which has led us to discover a surprising result that no existing work has achieved.

In this paper, we attempt to solve the theoretically challenging optimization problem.

- We establish a set of optimality properties for cases with stable energy harvesting, which characterize the necessary conditions for any optimal schedule.
- Our study reveals the surprising discovery that the optimal transmission power is independent of the transmission time but depends solely on the RF harvesting power. This discovery offers valuable insights for addressing related problems in the field.
- Additionally, we introduce an optimal offline HTT-scheduling for the general case that allows RF power to vary with time. To the best of our knowledge, it is the first optimal HTT-scheduling algorithm that achieves maximum data throughput for time-varying RF powered systems.
- We also present the design of an online heuristic algorithm aimed at maximizing throughput in RF power harvesting systems. Its superior performance compared with the optimal offline algorithm is demonstrated by simulations.

The remainder of this paper is organized as follows. In Section II, we formally define the system model and the optimization problem. A set of optimality properties for the *HTT-scheduling* is obtained and presented in Section III. An optimal scheduling algorithm for the defined problem is presented in Section IV and Section V. The online scheduling problem is investigated in Section VI, where an online algorithm is presented. Simulation results are also discussed in the same Section. Section VII concludes this paper. A few proofs of the algorithm have been omitted here because of space limitations, but they are available in an extended version [36].

II. PROBLEM FORMULATION

A. System Model

We consider a simple communication channel consisting of a data receiver and a wireless-powered data transmitter. The transmitter transmits data to the receiver over an AWGN wireless communication channel, which is widely adopted in the literatures [13], [15], and [16]. An outside power source, such as TV/WiFi broadcasting signal, cellular signal, or power beacon, is assumed to provide wireless power to the transmitter. Generally, the energy harvested from the outside power source is varying in time. The RF harvesting power is

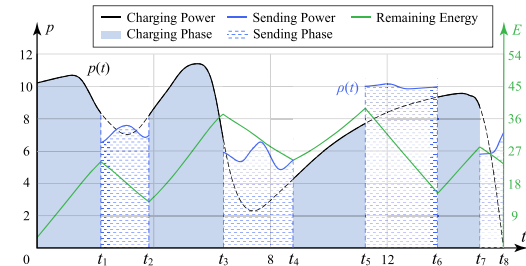


Fig. 2. A wireless transmitter harvests energy in the charging phases and transmits data in the sending phases. The charging power $p(t)$ is a time-varying function. The phase switching time t_i and the sending power $\rho(t)$ are to be determined to maximize throughput. Obviously, the remaining energy increases in the charging phases and decreases in the sending phases.

therefore a time-varying function, denoted as $p(t)$, $0 \leq t \leq T$, where T is the length of the duration in consideration.

The transmitter has to first harvest energy before it can transmit data, so the ‘harvest-then-transmit’ principle is used. We therefore define a two-phase cycle that consists of a charging phase and a sending phase. In the charging phase, the transmitter harvests the wireless power, and in the sending phase, it sends data to the receiver. The transmitter repeatedly and continuously switches between the two phases in the time interval $[0, T]$. Suppose that there are m cycles in this interval. Thus, there are $2m$ phases and $2m$ switches, which occur at time instances $\{t_1, t_2, \dots, t_{2m}\}$, $0 < t_1 < \dots < t_{2m}$. The $2m$ phases are labeled from 1 to $2m$, with phase i starting from time t_{i-1} and ends at t_i ($i = 1, 2, \dots, 2m$). The lengths of these phases are to be determined by our algorithm. However, it is assumed that there is a lower bound Δt for the length of any charging phase, which is imposed by the hardware.

Note that we assume $t_0 = 0$ and the battery has an initial energy E_{init} . Obviously, phase $2i-1$ is a charging phase, and phase $2i$ is a sending phase, $i = 1, 2, \dots, m$.

In sending phases, the transmission power is denoted as $\rho(t)$, which is subject to the *power constraint* of Eq. (1), where ρ_{max} is the maximum transmission power imposed by the hardware.

$$0 \leq \rho(t) \leq \rho_{max}, 0 \leq t \leq T. \quad (1)$$

At time t , the transmitter could choose one of the actions below:

- 1) Consume the energy of the battery at a given power $\rho(t)$ and transmit data.
- 2) Charge the battery with power $p(t)$. The minimum charging phase length is Δt , which is imposed by the hardware.

Fig. 2 illustrates the relations among the notations of the charging phase, the sending phase, the harvesting power (charging power), the transmission power (sending power), and the remaining energy.

B. Problem Formulation

Let $H(t)$ be the total energy charged into the battery before time t , which can be calculated as follows.

$$H(t) = \sum_{i=1}^{k-1} \int_{t_{2i-2}}^{t_{2i-1}} p(t) dt + \int_{t_{2k-2}}^{\min\{t, t_{2k-1}\}} p(t) dt,$$

where k satisfies $t_{2k-2} < t \leq t_{2k}$.

Let $E(t)$ be the total energy consumed before time t , which can be calculated as follows.

$$E(t) = \sum_{i=1}^{k-1} \int_{t_{2i-1}}^{t_{2i}} \rho(t) dt + \int_{\min\{t, t_{2k-1}\}}^{\min\{t, t_{2k}\}} \rho(t) dt,$$

where k satisfies $t_{2k-2} < t \leq t_{2k}$.

Let $R(t)$ be the remaining energy in the battery at time t ,

$$R(t) = E_{init} + H(t) - E(t).$$

We ensure that the remaining energy cannot be negative:

$$R(t) \geq 0, \quad \forall t \in [0, T]. \quad (2)$$

Because current technology cannot fully charge the battery wirelessly in a short time, the battery capacity is assumed to be large enough and can never be overcharged. Therefore, the battery capacity does not affect the performance of any schedule.

During the sending phase, the received signal at time t from the transmitter is given as

$$U_t = h_t X + N_t$$

where $N_t \sim \mathcal{CN}(0, 1)$ is the circularly-symmetric complex Gaussian noise at the AP with unit variance, and h_t denotes the channel fading coefficient. Accordingly, the transmission power $\rho(t)$ at time t is tightly related to the transmission rate $r(t)$ through the *power-rate* function of Eq. (3), as commonly assumed [13], [15], [16]

$$r(t) = \log(1 + |h_t|^2 \rho(t)). \quad (3)$$

Note that in some other related works, it is also common to assume $r(t) = \frac{1}{2} \log(1 + |h_t|^2 \rho(t))$, and our proposed method is easy to be extended to these cases. In fact, as long as $r''(t) < 0$, our main results of this paper hold, more details can be found in the next section. In this paper, we assume $|h_t| = 1$. As a consequence, the total amount of data transmitted during the entire time interval $[0, T]$ can be calculated by the following equation

$$B = \sum_{i=1}^m \int_{t_{2i-1}}^{t_{2i}} \log(1 + \rho(t)) dt. \quad (4)$$

Since we are maximizing the throughput over a fixed period of time, we can simplify the problem by considering the total amount of data transmitted as the throughput. Therefore, B in Eq. (4) represents the data throughput.

Definition 1 (The HTT-scheduling problem): Let $p(t), t \in [0, T]$ be the harvesting power, the HTT-scheduling problem is to determine the phase switching points $t_i, i = 1, 2, \dots, 2m$ and the transmission power $\rho(t)$ in sending phases, so that the data throughput B in Eq. (4) is maximized while satisfying the power constraint Eq. (1) and remaining energy constraint Eq. (2).

The HTT-scheduling problem of Definition 1 is called the offline case if the function $p(t), 0 \leq t \leq T$ is completely known before scheduling. It is called the online problem if $p(t)$ is not known until time t reaches the start time of a two-phase cycle.

Unless otherwise specified, we use watt as the unit for power, joule for energy, second for time, and KB for throughput.

III. THE *wopt* POWER

In this section, we introduce the notion of *wopt* power, which will play a key role in designing an optimal HTT schedule. We use a simplified *HTT-scheduling problem* to explain this notion.

Definition 2 (Basic HTT-scheduling problem): An HTT-scheduling problem with the following 2 assumptions is called basic HTT-scheduling problem. 1) The harvesting power $p(t)$ remains constant for the entire duration of $[0, T]$; and 2) there is no limit on the maximum transmission power ρ_{max} .

It is well-known that [12], [15], and [19] if the wireless transmitter does not harvest any energy but solely relies on the initial energy E_{init} for the entire duration of T , then, because of the concave property of the power-rate function Eq. (3), the optimal transmission power is

$$\rho = \frac{E_{init}}{T}, \quad (5)$$

which depends on both the initial energy and the length of the duration in consideration.

Now we consider the wireless device has another option: It can harvest RF power to charge the battery. In this case, if there are multiple charging phases, we can always move a later charging operation to an earlier time. Therefore, for this case, a single charging phase followed by a single sending phase will produce an optimal solution.

Let us discuss how to determine the switching point between these two phases. Suppose that the phase-switching point is t_1 . Because a single constant transmission power ρ should be used in the sending phase, we obtain the following equation.

$$E_{init} + pt_1 = \rho(T - t_1).$$

Therefore,

$$t_1 = \frac{\rho T - E_{init}}{\rho + p}. \quad (6)$$

Since the data transmission rate is $\log(1 + \rho)$ at transmission power ρ , the total throughput B can be calculated by $B = (T - t_1) \log(1 + \rho)$. Plugging in the expression (6) for t_1 , we obtain the following function (7) for B . Clearly, it is a function of variable ρ .

$$B(\rho) = (pT + E_{init}) \frac{\log(1 + \rho)}{p + \rho}. \quad (7)$$

To help understand the function $B(\rho)$, we illustrate its shape in Fig. 3(a) when $p = 10$, $E_{init} = 7.6$ and $T = 8$. It can be seen that there is a maximum value of $B(\rho)$ for $\rho \in [0, 30]$. To analytically locate the maximum value of function $B(\rho)$, we calculate its first and second order of derivatives as shown below.

$$\begin{aligned} B'(\rho) &= (pT + E_{init}) \left(\frac{\log(1 + \rho)}{p + \rho} \right)' \\ &= \frac{pT + E_{init}}{(p + \rho)^2} \left[\left(1 + \frac{p - 1}{1 + \rho} \right) \frac{1}{\ln 2} - \log(1 + \rho) \right]. \end{aligned}$$

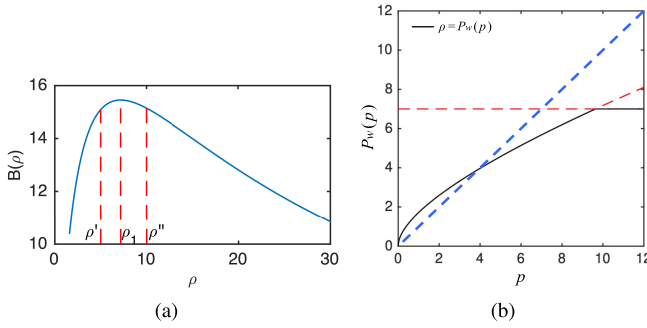


Fig. 3. (a) The shape of $B(\rho)$ in Eq. (7) when $p = 10$, $E_{init} = 7.6$ and $T = 8$, which is maximized at $\rho_w \approx 7.2$ and the phase switching time in Eq. (6) is $t_1 = 2.9$. (b) The curve of function $\rho = P_w(p)$ when $\rho_{max} = 7$.

Because $(pT + E_{init})/((p+\rho)^2) > 0$, we define function $g(\rho)$ as

$$\begin{aligned} g(\rho) &= B'(\rho)/\frac{pT + E_{init}}{(p+\rho)^2} \\ &= \left(1 + \frac{p-1}{1+\rho}\right)\frac{1}{\ln 2} - \log(1+\rho). \end{aligned}$$

Obviously, for any given ρ , $g(\rho)$ and $B'(\rho)$ share the same sign and zero point. Because

$$\begin{aligned} g'(\rho) &= -\frac{p-1}{(1+\rho)^2 \ln 2} - \frac{1}{(1+\rho) \ln 2} \\ &= -\frac{p+\rho}{(1+\rho)^2 \ln 2} < 0, \end{aligned}$$

$g(\rho)$ monotonically decreases. Hence $B(\rho)$ is concave and its maximum value can be found at point ρ_w , such that $g(\rho_w) = 0$. By setting $g(\rho_w) = 0$ we have the following derivations:

$$\begin{aligned} \left(1 + \frac{p-1}{1+\rho_w}\right)\frac{1}{\ln 2} &= \log(1+\rho_w), \\ \text{EXP}\left(1 + \frac{p-1}{1+\rho_w}\right) &= 1 + \rho_w, \\ \frac{p-1}{1+\rho_w} \text{EXP}\left(\frac{p-1}{1+\rho_w}\right) &= \frac{p-1}{e}, \\ \mathcal{W}\left(\frac{p-1}{e}\right) &= \frac{p-1}{1+\rho_w}, \end{aligned}$$

where function $\mathcal{W}(z)$ is called the Lambert W function [25], which has the following property,

$$\mathcal{W}(z)\text{EXP}(\mathcal{W}(z)) = z.$$

Therefore, we have

$$\rho_w = \frac{p-1}{\mathcal{W}\left(\frac{p-1}{e}\right)} - 1. \quad (8)$$

Fig. 3(a) shows an example of the function $B(\rho)$. Since $\rho_w \approx 7.2$ for this example, $t_1 = \frac{\rho_w T - E_{init}}{p+\rho} = \frac{7.2 \times 8 - 7.6}{10 + 7.2} = 2.9$.

From Eq. (6), we observe that, if $\rho T \leq E_{init}$, then t_1 should be 0 or negative, which means no charging is needed. We state the main result in the following lemma, whose correctness follows directly from the above discussion.

Lemma 1: If $E_{init} \leq \rho_w T$, then the optimal solution for the basic problem in Definition 2 consists of a charging phase and a sending phase. The phase transmission power is $\rho = \rho_w$

determined by Eq. (8) and switching point is t_1 determined by Eq. (6). If $E_{init} \geq \rho_w T$, then no charging phase is needed, and the transmission power is determined by Eq. (5).

We further have the following important theorem, despite the optimal charging/sending phase switching point, namely t_1 from Eq. (6), depends on E_{init} , p and T .

Theorem 1: The optimal sending power ρ_w is independent of E_{init} and T , and depends only on the harvesting power p when $E_{init} \leq \rho_w T$.

This theorem is quite surprising. It plays a key role in the optimal solutions for the general HTT-scheduling problem defined in Definition 1.

Some previous work in the literatures [15] and [19] also studied the same basic problem, but they all failed to discover Theorem 1 because they focused on finding the optimal phase length t_1 , while we, instead, focus on computing the optimal transmission power ρ . In a recent attempt by Zewde and Gursoy [15], the optimal harvesting time from Eq. (25) in [15],

$$t_B^* = \frac{e^{\mathcal{W}\left(\frac{p-1}{e}\right)+1} - 1}{p + e^{\mathcal{W}\left(\frac{p-1}{e}\right)+1} - 1}, \quad (9)$$

is a specially case of our optimal phase switching time t_1 from Eq. (6) by setting $\rho = \rho_w$,

$$t_1 = \frac{\rho_w T - E_{init}}{p + \rho_w} = \frac{\left(\frac{p-1}{\mathcal{W}\left(\frac{p-1}{e}\right)} - 1\right)T - E_{init}}{p + \frac{p-1}{\mathcal{W}\left(\frac{p-1}{e}\right)} - 1}. \quad (10)$$

Note that $e^{\mathcal{W}\left(\frac{p-1}{e}\right)+1} = \frac{p-1}{\mathcal{W}\left(\frac{p-1}{e}\right)}$ by the definition of the Lambert W function. When $T = 1$ and $E_{init} = 0$, our result Eq. (10) can be reduced to their result Eq. (9). However, we instead, focus on the optimal transmission power, which leads to the surprising new discovery in Theorem 1. Our discovery reveals an essential property of RF powered data transmission that has never been disclosed before.

We now introduce the *wopt* power in preparation for the general case, where the wireless power p may change from time to time.

Definition 3 (wopt power $P_w(p)$): For any given harvesting power p , the wopt power $P_w(p)$ is defined as follows.

$$P_w(p) = \min\left\{\frac{p-1}{\mathcal{W}\left(\frac{p-1}{e}\right)} - 1, \rho_{max}\right\}, \quad (11)$$

where ρ_{max} is the maximum available transmission power which is imposed by the hardware.

The function $P_w(p)$ is the most important concept throughout this paper. Fig. 3(b) shows the curve of this function for the range of $p \in (0, 12)$ and $\rho_{max} = 7$ to give the reader an intuitive idea of this function. For any given wopt power ρ which is less than ρ_{max} , we can compute its inverse function to obtain the harvesting power $p = P_w^{-1}(\rho)$.

IV. AN OPTIMAL OFFLINE SOLUTION FOR DECREASING HARVESTING POWER

In this section and in the following section, we will develop an optimal offline algorithm for the HTT-scheduling problem defined in Definition 1, which is the basis of the algorithm for the general case investigated in the next section. In this

section, we solve a simpler case where the harvesting power function $p(t)$ is assumed to be monotonically decreasing.

Before we design the algorithm that computes the optimal solution, we first want to see what the optimal solution should be like. We therefore present the following theorems on the optimal solution.

Theorem 2: For HTT-scheduling problem, when the harvesting power $p(t)$ is monotonically decreasing, there exists an optimal solution in which a power level w exists such that (1) in any charging phase we have $p(t) > w$, (2) in any sending phase we have $p(t) \leq w, 0 \leq t \leq T$. The level w is called the dam height.

Theorem 3: In the optimal solution, when the harvest power $p(t)$ is monotonically decreasing, the sending power of the sending phase should be $P_w(w)$, where w is the dam height.

Theorem 2 and 3 are special cases of Theorem 5 and 6, respectively. Due to space constraints, we provide the full proofs in the extended version of this paper [36].

From Theorem 2 and Theorem 3, we have known that there is an important *dam height*, which not only distinguishes charging phases from sending phases but also determines the sending power. Therefore, once the optimal *dam height* is determined, the HTT schedule is determined.

Definition 4 (Dam w HTT-schedule): Given the harvesting power $p(t)$ and the initial battery energy E_{init} , the following scheduling is called the Dam w HTT-schedule.

- Any charging phase $[a, b]$ satisfies $p(t) \geq w, t \in [a, b]$.
- Any sending phase $[c, d]$ satisfies $p(t) \leq w, t \in [c, d]$, and its sending power is $P_w(w)$.

Note that, inside either phase, we may have $p(t) = w$. This could occur especially when $p(t)$ is a constant function.

Now the only question is how to find the optimal *dam height* w_{opt} such that the Dam w_{opt} HTT-schedule maximizes data throughput before T .

We start from the following lemma, which is obviously true with no need of proof.

Lemma 2: In a Dam w HTT-schedule, when the dam height w increases, the energy used in sending increases, while charged energy decreases as charging phases shrink, hence the remaining energy $R(T)$ reduces monotonically.

Since in the optimal HTT-schedule, there must be no remaining energy in the battery at the ending time T , our strategy is to search the optimal *dam height* w_{opt} such that in the Dam w_{opt} HTT-schedule, $R(T) = 0$.

We hence design the *dam raising system* to find the optimal *dam height*. Such a system is built upon the time-power diagram, as presented in Fig. 4. Note that in this diagram, we introduce a virtual phase with a virtual harvesting power $p(t) = w_{max}$, where $w_{max} = P_w^{-1}(\rho_{max})$, $t \in [-E_{init}/w_{max}, 0]$. This virtual phase is to pre-charge the battery to E_{init} .

We now introduce the *dam raising system* on the time-power diagram in Fig. 4. The curve of $p(t)$ is treated as a mountain. Although in the current decreasing harvesting power case, there is only one downslope, our system is intended for general $p(t)$ where both downslopes and upslopes exist, i.e., there are hills and valleys. In this mountain area, we want to build a dam to hold water (in the valley and underground).

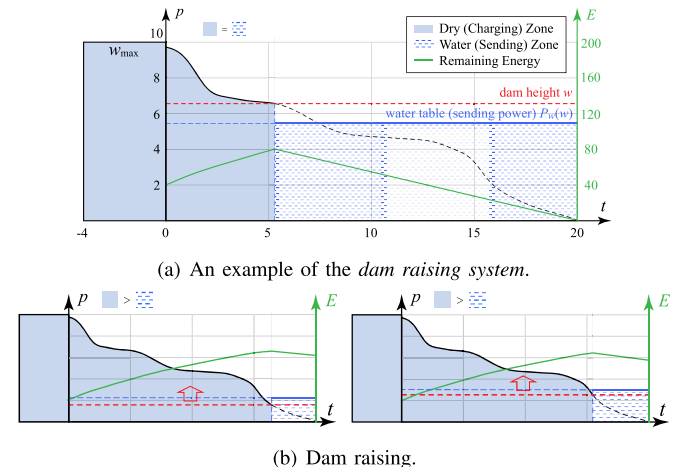


Fig. 4. An example of the *dam raising system* and how the dam is raised. (a) The *dam raising system* is introduced on the time-power diagram, where the curve of $p(t)$ is treated as a mountain (especially for the general $p(t)$). In this mountain area, a dam is built to hold water. A dam with height w can hold the water table with height $P_w(w)$ (see Section III). The dam height w divides the mountain area into hills and valleys. Only the valley and its underground hold water, no water beneath the surfaces of the hill. The area right beneath the surface of the hill is called the dry zone (charging zone), whose area is actually the amount of energy charged into the battery; the area right beneath the water table is called the water zone (sending zone) whose area is actually the energy consumed for sending data. (b) In the *dam raising system*, the dam height w is raised slowly to find its optimal position. It starts with $w = 0$ and stops raising as soon as the dry zone area equals the water zone area. The green curve indicates the remaining energy in the battery, which increases during the charging phase and decreases during the sending phase.

Assume a dam with height w can hold the water table with height $P_w(w)$. The dam height w divides the mountain area into hills and valleys. Only the valley and its underground hold water, no water beneath the surface of the hill. The area right beneath the surface of the hill is called *dry zone*; the area right beneath the water table is called the *water zone*. The dam has the maximum height $P_w^{-1}(\rho_{max})$ and the water table has the maximum height ρ_{max} . Hence, the virtual phase is guaranteed to be a charging phase in our system.

Since an area on the time-power diagram represents an amount of energy, the *dry zone* area corresponds to the energy harvested into the battery, while the *water zone* area corresponds to the energy consumed in sending data. Therefore, the difference between the two zone areas is the remaining energy $R(T)$. In Fig. 4, the green curve with its corresponding right y-axis indicates the remaining energy in the battery, which increases during the charging phase and decreases during the sending phase.

The core of the *dam raising system* is to raise the dam height from $w = 0$, and stop as soon as the dry zone area equals the water zone area. Then the optimal dam height and the optimal water table are found. At the very beginning, the entire area is a dry zone with no water zone. As the dam height is raised, the dry zone shrinks horizontally, while the water zone grows both horizontally and vertically. Hence, a unique dam height can be found that equals the two zone areas. The dam raising stops at this height.

For any *Dam w HTT-schedule*, it is easy to compute the remaining energy $R(t)$ at any time $t \in [0, T]$. And $R(t)$ is

illustrated by the green remaining energy curve on the diagram in Fig. 4. Let a procedure $\text{is_shortage}(t_s, t_e, E_0, w)$ checks whether any part of the remaining energy curve in duration $[t_s, t_e]$ goes below 0 which means energy shortage and infeasible schedule, where E_0 is the initial energy for $[t_s, t_e]$, and w is the dam height. The procedure returns *true* if there is any shortage, *false* if the schedule is feasible. Obviously, the time complexity of this check is $O(|t_e - t_s|)$. Hence, we want to find the highest dam height w such that $\text{is_shortage}(0, T, E_{\text{init}}, w)$ returns *false*.

In the formal algorithm, the process of dam raising can be efficiently speeded up by bisection searching. Algorithm `dam_raising_shotg` provides formal details.

A simple call to `dam_raising_shotg(0, T, Einit)` will return the optimal dam height.

Theorem 4: Algorithm `dam_raising_shotg(0, T, Einit)` computes the optimal HTT schedule, and time complexity of the algorithm is $O(T \cdot \log(\frac{\rho_{\max}}{\Delta}))$, where Δ is the desired accuracy.

Proof: See Appendix A. \square

V. THE OPTIMAL OFFLINE SOLUTION FOR GENERAL HARVESTING POWER

The section focuses on the general harvesting power case and extends results for the special case of the monotonically decreasing harvesting power. Before we design the algorithm that computes the optimal solution, we first present the following theorems on the optimal solution. It is not hard to see that the following theorems are similar to those in the previous section.

Theorem 5: For the general HTT-scheduling problem, when the harvesting power $p(t)$ is a general function, in the optimal schedule, there exists a set of time τ_i , and the power level w_i for interval $[\tau_{i-1}, \tau_i]$, in which (1) for any charging phase, we have $p(t) > w_i$, (2) for any sending phase, we have $p(t) \leq w_i, 0 \leq t \leq T, i = 1, 2, \dots, n$, unless $p(t)$ monotonically increases in $[\tau_{i-1}, \tau_i]$. The power level w_i is called the dam heights.

Proof: See Appendix B. \square

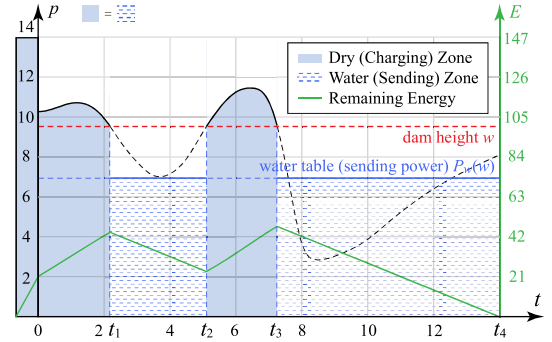
Lemma 3 (Expanding and shrinking): Suppose w and ρ are the dam height and sending power in a sending phase. If $P_w(w) < \rho$ ($P_w(w) > \rho$) satisfies, then there exists an operation that expands (shrinks) a sending phase via including

Algorithm 1 `dam_raising_shotg(ts, te, E0)`

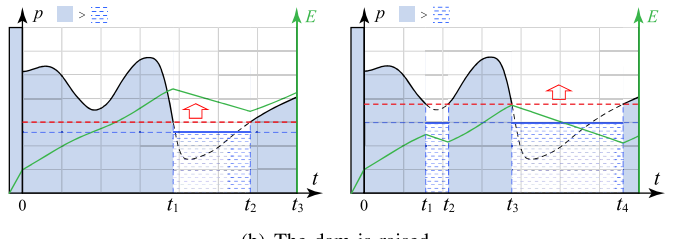
```

1  $w_{\text{lower}} = 0;$ 
2  $w_{\text{upper}} = \rho_{\max};$ 
3 while  $w_{\text{upper}} - w_{\text{lower}} > \Delta$  do
4    $w = \frac{w_{\text{upper}} + w_{\text{lower}}}{2};$ 
5   if  $\text{is\_shortage}(0, T, E_{\text{init}}, w) = \text{false}$  then
6     |  $w_{\text{lower}} = w$ 
7   else
8     |  $w_{\text{upper}} = w$ 
9   end
10 end
11 return  $w$ 

```



(a) The *dam raising system* for general harvesting power.



(b) The dam is raised.

Fig. 5. The dam is raised in the *dam raising system* for general harvesting power. (a) For general $p(t)$, there are more than one dry zone and water zones. However, all underground water is connected, so they share the same water table in all valleys. (b) When the dam is raised, the water table rises too. The dam raising will create new valleys and open new water zones. As the dam height w grows larger, the green remaining energy curve increases less but decreases in a larger slope, as a result, this curve generally becomes lower in position. We stop raising once the green curve touches the x-axis because that means the battery is energy-critical at the touch point.

(excluding) a small duration at both ends while meeting the following constraints.

- The operation doesn't change the energy consumption.
- The operation doesn't decrease the throughput.

Proof: See Appendix C. \square

Theorem 6: In any sending phase of the optimal HTT schedule, the sending power is $P_w(w)$, where w is the dam height of the sending phase.

Proof: See Appendix D. \square

Due to the similarity between these theorems and the theorems in the previous section, *dam raising system* can be conveniently extended to the general $p(t)$ function. Recall that the dam height is raised slowly (so as the water table), and the dam height stops rising once the dry zone area equals the water zone area, which indicates the harvesting energy is used up in sending data. The dam height and water table are raised exactly the same way for the general $p(t)$ function. One of the differences is that there may be more than one dry zone and more than one water zone. The dam height will meet each valley in order when it rises. When the dam height is raised, the total dry zone area grows, but the total water zone area shrinks, e.g., Lemma 2 still holds. We stop when the two areas are equal. We define such a revised algorithm `dam_raising_general`. This algorithm is executed on the part of the $p(t)$ from Fig. 2, and the results are given in Fig. 5.

However, the biggest difference for the general $p(t)$ function is that it is not always possible that one dam height can make the dry zone area be equal to the water zone area. If we

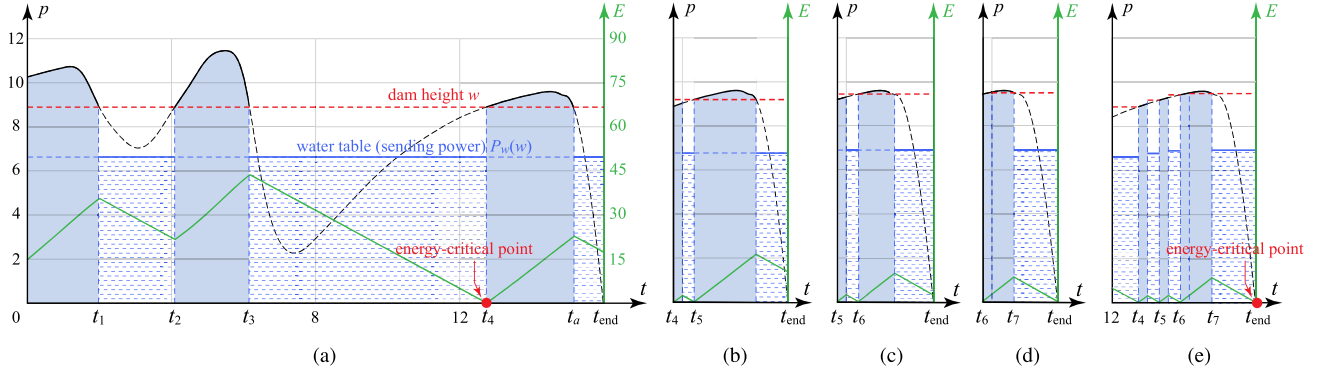


Fig. 6. The *dam raising system* may generate multiple dam heights. (a) The dam height is slowly raised to the highest position that is feasible. In such a position, there must be an energy-critical point so that further raising will cause an energy shortage. The dam height before such a point is optimal. (b) Once the battery is energy-critical (t_4 at (a)), we charge the battery for Δt time. Starting at this point, the same problem repeats. In this new problem, the remaining energy curve will not touch the x-axis until the dam continues to be raised above $p(t_4)$. This is called the fast switching cycle. (c) A number of adjacent fast switching cycles follow, and they are called the fast switching period. (d) When the dam continues to be raised above $p(t_6)$, the first energy-critical point that appears is t_{end} . Therefore, the fast switching period ended. (e) Full view of the fast switching period. The fast switching period begins at t_4 and ends at t_6 , and there are 2 fast switching cycles in the fast switching period: $t_4 \sim t_5$ and $t_5 \sim t_6$.

consider a longer $p(t)$ function from Fig. 2, then the problem arises. As in Fig. 6(a), since the dry zone in $[t_4, t_a]$ is larger than the following water zone, the total area of the dry zone is larger than that of the water zone. We may want to raise the dam to enlarge the charging zone and shrink the sending zone. However, the raise is impossible, because we already have the two zones equal before time t_4 , i.e., the green remaining energy curve touches the x-axis at time t_4 . Note that although $R(t_4) = 0$, there is still a certain amount of energy at time t_4 to keep the device functional which is not considered in the *dam raising system* design. So there is no single dam height for the entire duration $[0, T]$ such that the two zones before T are equal.

In conclusion, throughout the entire duration $[0, T]$, the optimal dam height does not necessarily stay unchanged. Instead, it may change multiple times. Assume it changes at time $t = \tau_i, i = 1, 2, \dots, n$, and stays constant in all adjacent cycles in $[\tau_{i-1}, \tau_i]$ at w_i . Now, the problem becomes how to find all the dam height w_i and the dam height changing points $\tau_i, i = 1, 2, \dots, n$.

Before we go any further with the algorithm, we first investigate some optimality properties of the optimal dam height.

Lemma 4: Any two distinct dam heights from two disjoint durations can be equalized to transmit more data in these two durations, unless infeasible solution results.

Proof: See Appendix E. \square

Lemma 5: The optimal dam height increases only.

Lemma 6: The optimal dam height increases at energy-critical points.

The proofs of Lemma 5 and Lemma 6 can be obtained by applying Lemma 4. Due to space limitations, the details are provided in the extended version of this paper [36].

The battery must be charged once it is energy-critical, the following definitions state what is the energy-critical point and how it is charged in the optimal solution.

Definition 5 (The energy-critical point): If at time point t the energy in the battery available for transmitting the data is 0, then the time point t is an energy-critical point.

Note that, at an energy-critical point, there is only a little energy that keeps the device functional remains and there's no energy available for transmitting the data.

Immediately following an optimal energy-critical point, there must be a charging phase with length at least length Δt , where Δt is the minimum time required for a device to stay harvesting which is imposed by the hardware.

Definition 6 (The fast switching cycle and fast switching period): A cycle is called the fast switching cycle if its charging phase is with length Δt , and the sending phase uses up all the energy in the battery. Adjacent fast switching cycles are called a fast switching period.

Note that an example of the optimal solution that satisfies all the above Lemma 5, 6 and Definition 6 is given in Appendix F.

We are now ready to present the algorithm. The high level idea is quite simple, we want to find the first dam height changing point for the optimal dam height and after such a point, the same problem repeats. According to Lemma 6, 1) at such a point, the battery is energy-critical, and 2) before such a point, there is a single dam height, and 3) after such a point, the dam height increases. Hence, we find the largest dam height w for the entire duration that is feasible with an energy-critical point. We will prove later that such a point is the first optimal dam height changing point, and the dam height w is also optimal before such a point.

We can call the previously introduced `dam_raising_shotg` to directly return such a dam height w . Let the procedure of finding the energy-critical point for w be `find_emptyP(t_s, t_e, E_0, w)`, where $[t_s, t_e]$ is the duration in consideration, E_0 is the initial energy for such duration, and w is the given dam height. The procedure returns the first energy-critical point τ if it exists. Starting from τ , we charge the battery for Δt time, and charge $\int_{t=\tau}^{\tau+\Delta t} p(t) dt$ energy into the battery. The point $\tau + \Delta t$ will be treated as the new starting point for the next iteration.

Algorithm `Varying_Source_WPT` computes all the changing points and the dam heights.

Theorem 7: The algorithm `Varying_Source_WPT` computes the optimal schedule for the offline problem, and the time complexity of the algorithm is $O(T^2 \log(\frac{\rho_{\max}}{\Delta}) / \Delta t)$.

Algorithm 2 Varying_Source_WPT

```

1  $\tau_0 = 0, E_0 = E_{init}$ ;
2 while  $\tau_0 < T$  do
3    $w = \text{dam\_raising\_shotg}(\tau_0, T, E_0)$ ;
4    $\tau = \text{find\_emptyP}(\tau_0, T, E_0, w)$ ;
5   Set dam height  $w$  in  $[\tau_0, \tau]$ ;
6    $\tau_0 = \tau + \Delta t, E_0 = \int_{t=\tau}^{\tau+\Delta t} p(t) dt$ ;
7 end
```

Proof: See Appendix G. \square

An example of the execution of Algorithm Varying_Source_WPT is illustrated in Fig. 6. By line 3, we slowly raise the dam height w and the corresponding water table $P_w(w)$.

As the dam height w grows larger, the green *remaining energy curve* increases less but decreases in a larger slope, as a result, this curve generally becomes lower in position. Once the dam height w is raised to a height that causes the curve to touch the x-axis, we stop, because that means the battery is energy-critical at the touch point. Line 3 returns this height w and line 4 returns the time of the touch point τ . We have proved such dam height is optimal. Note that, since the battery is energy-critical at τ , according to Definition 6, we set interval $[\tau, \tau+\Delta t]$ to charge the battery, and the charged energy $E_0 = \int_{t=\tau}^{\tau+\Delta t} p(t) dt$. In Fig. 6(b), the *remaining energy curve* will not touch the x-axis until the dam height continues to rise above $P(t_4)$. Since the previous charging phase length Δt is small, the initial energy $E_0 = \int_{t=\tau}^{\tau+\Delta t} p(t) dt$ is small, so with a small sending phase, the curve touches x-axis, and we stop. This is called the *fast switching cycle*, obviously, there will be fast switches in this period among harvesting and transmitting phases. The *fast switching period* may last for a number of more cycles, like in Fig. 6(c). In Fig. 6(d), when the dam continues to be raised above $p(t_6)$, the first energy-critical point that appears is t_{end} . Therefore, the fast switching period ended. Fig. 6(d) gives a full view of the fast switching period. The fast switching period starts from t_4 and ends at t_6 . There are 2 fast switching cycles in the period: $t_4 \sim t_5$ and $t_5 \sim t_6$.

A more complicated example with three dam heights and two *fast switching periods* is given in Appendix F.

VI. ONLINE ALGORITHM AND SIMULATIONS

In this section, we study the online *HTT-scheduling* problem, where the phase switching points and the transmission power are determined based on the past and current harvesting power, *i.e.*, any $p(t)$ is not known until time t . We propose a heuristic algorithm, namely *dam guided online algorithm*, which is based on the optimal properties obtained from the offline problem. We then provide some basic theoretical analysis of this online algorithm. Finally, performance evaluation is conducted by comparisons with the optimal offline solutions.

A. Online Algorithm

The core idea of *dam guided online algorithm* is to use the history average harvesting power to anticipate any

TABLE I
SUMMARY OF ONLINE SETTINGS TO l_1 AND l_2

	$\frac{\bar{p}}{p+P_w(\bar{p})} \geq 1$	$\frac{1}{2} < \frac{\bar{p}}{p+P_w(\bar{p})} < 1$	$\frac{\bar{p}}{p+P_w(\bar{p})-\bar{p}} \leq \frac{1}{2}$
l_1	0	Δt	$\frac{\bar{p}}{p+P_w(\bar{p})-\bar{p}} \Delta t$
l_2	Δt	$\frac{\bar{p}}{p+P_w(\bar{p})-\bar{p}} \Delta t$	Δt

unknown further harvesting power and compute the next charging-sending cycle based on the current harvesting power. Meanwhile, we do not want the next cycle to last too long, because harvesting power is time-varying and we have no future information. We want the cycle to be as short as possible.

More specifically, assume at the current time t , the charging power is p and the battery energy is E_r , while the history average charging power is \bar{p} . Suppose l_1 , l_2 , and ρ are the lengths of the charging phase, sending phase, and the sending power respectively, which are to be determined by the online algorithm.

A total of $(l_1 + l_2)\bar{p}$ energy is expected to be harvested on average in the next cycle if both phases are used for charging. If we set the sending power to be $P_w(\bar{p})$ in the second phase, then compared with the both phase charging case, this sending phase not only costs $l_2 P_w(\bar{p})$ energy in sending data, but also costs $l_2 \bar{p}$ energy less charged into the battery. Therefore, the remaining energy is $(l_1 + l_2)\bar{p} - (l_2 P_w(\bar{p}) + l_2 \bar{p}) = l_1 \bar{p} - l_2 P_w(\bar{p})$, *i.e.*, the sum of both cost should be deducted.

As long as l_1 and l_2 are small enough, we can treat harvesting power as a constant, which is p . Then, the sending phase with length l_2 costs $l_2 P_w(\bar{p}) + l_2 p$ energy loss, including $l_2 P_w(\bar{p})$ energy consumed and $l_2 p$ energy less charged. We want the energy loss to equal to the expected energy harvesting, *e.g.*, $(l_1 + l_2)\bar{p} = l_2(P_w(\bar{p}) + p)$ because the energy charged and energy consumed should equal in a long run. Therefore, l_1 and l_2 satisfies

$$\frac{l_2}{l_1 + l_2} = \frac{\bar{p}}{p + P_w(\bar{p})}. \quad (12)$$

Obviously, only if $\frac{\bar{p}}{p+P_w(\bar{p})} < 1$, then $l_1 > 0$. Hence, we set $l_1 = 0$ and $l_2 = \Delta t$ when $\frac{\bar{p}}{p+P_w(\bar{p})} \geq 1$. When $\frac{1}{2} < \frac{l_2}{l_1+l_2} < 1$, l_1 is smaller than l_2 , we hence set $t_1 = \Delta t$ and compute l_2 accordingly, $l_2 = \frac{\bar{p}}{p+P_w(\bar{p})-\bar{p}} \Delta t$. When $\frac{l_2}{l_1+l_2} \leq \frac{1}{2}$, l_2 is smaller, hence we set $l_2 = \Delta t$ and $l_1 = \frac{p+P_w(\bar{p})-\bar{p}}{\bar{p}} \Delta t$. These settings to l_1 and l_2 are summarized in Table I.

The Algorithm *dam_guided_online* presents the detailed pseudo code.

B. The Basic Theoretical Analysis

The general idea of our basic theoretical analysis is, we take two general intervals and analysis the throughput and energy usage within both intervals. Assume the time-varying harvesting power function $p(t), 0 \leq t \leq T$ has the average power at \bar{p} , then the two taken intervals must also average to \bar{p} , otherwise, they are not general enough. Let them be called interval x and interval y , both with length L . If x and y both have harvesting powers equal to \bar{p} , then it is quite straightforward to check

Algorithm 3 dam_guided_online(E_r, t, p)

```

1 Update the average harvesting power  $\bar{p}$ ;
2 if  $\frac{p+P_w(\bar{p})}{\bar{p}} \leq 1$  then
3   |    $l_1 = 0$ ;
4   |    $l_2 = \Delta t$ ;
5 else if  $1 < \frac{p+P_w(\bar{p})}{\bar{p}} \leq 2$  then
6   |    $l_1 = \Delta t$ ;
7   |    $l_2 = \frac{\bar{p}}{p+P_w(\bar{p})-\bar{p}} \Delta t$ ;
8 else if  $2 < \frac{p+P_w(\bar{p})}{\bar{p}}$  then
9   |    $l_1 = \frac{p+P_w(\bar{p})-\bar{p}}{\bar{p}} \Delta t$ ;
10  |    $l_2 = \Delta t$ ;
11 end
12 if  $E_r + l_1 p - l_2 P_w(\bar{p}) < 0$  then
13   |    $l_2 = 0$ ;
14 end
15 Set charging phase  $[t, t + l_1)$ ;
16 Set sending phase  $[t + l_1, t + l_1 + l_2)$ , and sending power
 $P_w(\bar{p})$ ;
```

that the proposed online algorithm produces a solution with throughput equal to the offline optimal solution.

We therefore focus on the cases when harvesting power in the two intervals varies. Assume $p(t)$ is bounded by $p_{min} \leq p(t) \leq p_{max}$, $0 \leq t \leq T$, and $p_{min} = (1 - \gamma)\bar{p}$ and $p_{max} = (1 + \gamma)\bar{p}$, where γ represents the deviation of variation. We study the case where the two taken intervals have the largest variation deviation of $p(t)$ because the throughput and energy usage are affected the most. Without loss of generality, we assume the harvesting power $p = (1 - \gamma)\bar{p}$ in interval x and $p = (1 + \gamma)\bar{p}$ in interval y , and x is before y . We will show next the throughput and energy usage differences between a simple offline solution and the online solution by the proposed online algorithm.

Assume in an offline solution, all energy harvested is used up in x and y , respectively, that is

$$E^{off} = 0.$$

Then, according to the constant harvesting power analysis in Section III and Eq. (7), we have the throughput for this offline solution as follows,

$$\begin{aligned} E^{off} &= (1 - \gamma)\bar{p}L \frac{\log(1 + P_w((1 - \gamma)\bar{p}))}{(1 - \gamma)\bar{p} + P_w((1 - \gamma)\bar{p})} \\ &\quad + (1 + \gamma)\bar{p}L \frac{\log(1 + P_w((1 + \gamma)\bar{p}))}{(1 + \gamma)\bar{p} + P_w((1 + \gamma)\bar{p})}. \end{aligned} \quad (13)$$

Since function $B^{on}(p) = pL \frac{\log(1 + P_w(p))}{p + P_w(p)}$ is a concave function, so according to Jensen's inequality, we have

$$E^{off} \leq 2\bar{p}L \frac{\log(1 + P_w(\bar{p}))}{\bar{p} + P_w(\bar{p})}. \quad (14)$$

We now study the throughput and energy usage of the online solution produced by the proposed online algorithm. Since the online algorithm produces cycles with very small lengths, we first investigate the length percentage of both phases. Since the sending phase length percentage has already been

presented in Eq. (12), the charging phase length percentage is therefore $\frac{l_1}{l_1+l_2} = 1 - \frac{\bar{p}}{p+P_w(\bar{p})}$. Therefore, we have

$$\begin{aligned} \frac{l_{x1}}{l_{x1} + l_{x2}} &= 1 - \frac{\bar{p}}{(1 - \gamma)\bar{p} + P_w(\bar{p})}, \quad l_{x1} + l_{x2} = L \\ \frac{l_{y1}}{l_{y1} + l_{y2}} &= 1 - \frac{\bar{p}}{(1 + \gamma)\bar{p} + P_w(\bar{p})}, \quad l_{y1} + l_{y2} = L \end{aligned}$$

Therefore,

$$\begin{aligned} l_{x2} &= \frac{\bar{p}}{(1 - \gamma)\bar{p} + P_w(\bar{p})}L \\ l_{y2} &= \frac{\bar{p}}{(1 + \gamma)\bar{p} + P_w(\bar{p})}L \end{aligned}$$

The throughput of the solution by our online algorithm is the sum of all data sent in every sending phase in both intervals x and interval y .

$$\begin{aligned} B^{on} &= l_{x2} \log(1 + P_w(\bar{p})) + l_{y2} \log(1 + P_w(\bar{p})) \\ &= \frac{\bar{p}}{(1 - \gamma)\bar{p} + P_w(\bar{p})}L \log(1 + P_w(\bar{p})) \\ &\quad + \frac{\bar{p}}{(1 + \gamma)\bar{p} + P_w(\bar{p})}L \log(1 + P_w(\bar{p})). \end{aligned}$$

Since function $B^{off}(p) = \bar{p}L \frac{\log(1 + P_w(\bar{p}))}{p + P_w(\bar{p})}$ is a concave function, so

$$B^{on} \geq 2\bar{p}L \frac{\log(1 + P_w(\bar{p}))}{\bar{p} + P_w(\bar{p})}. \quad (15)$$

Therefore,

$$B^{on} \geq B^{off}. \quad (16)$$

The energy harvested into the system by our online algorithm in charging phases of both x and y is

$$\begin{aligned} E_{in}^{on} &= (1 - \frac{\bar{p}}{(1 - \gamma)\bar{p} + P_w(\bar{p})})L(1 - \gamma)\bar{p} \\ &\quad + (1 - \frac{\bar{p}}{(1 + \gamma)\bar{p} + P_w(\bar{p})})L(1 + \gamma)\bar{p} \\ &= L\bar{p}(\frac{(1 - \gamma)(1 - \gamma \frac{\bar{p}}{P_w(\bar{p})})}{(1 - \gamma) \frac{\bar{p}}{P_w(\bar{p})} + 1} + \frac{(1 + \gamma)(1 + \gamma \frac{\bar{p}}{P_w(\bar{p})})}{(1 + \gamma) \frac{\bar{p}}{P_w(\bar{p})} + 1}). \end{aligned}$$

The energy consumed in the sending phases of both intervals is

$$\begin{aligned} E_{out}^{on} &= \frac{\bar{p}}{(1 - \gamma)\bar{p} + P_w(\bar{p})}LP_w(\bar{p}) \\ &\quad + \frac{\bar{p}}{(1 + \gamma)\bar{p} + P_w(\bar{p})}LP_w(\bar{p}) \\ &= L\bar{p}(\frac{1}{(1 - \gamma) \frac{\bar{p}}{P_w(\bar{p})} + 1} + \frac{1}{(1 + \gamma) \frac{\bar{p}}{P_w(\bar{p})} + 1}). \end{aligned}$$

So,

$$\begin{aligned} E^{on} &= E_{in}^{on} - E_{out}^{on} = L\bar{p}(\frac{-\gamma - \gamma \frac{\bar{p}}{P_w(\bar{p})} + \gamma^2 \frac{\bar{p}}{P_w(\bar{p})}}{(1 - \gamma) \frac{\bar{p}}{P_w(\bar{p})} + 1} \\ &\quad + \frac{\gamma + \gamma \frac{\bar{p}}{P_w(\bar{p})} + \gamma^2 \frac{\bar{p}}{P_w(\bar{p})}}{(1 + \gamma) \frac{\bar{p}}{P_w(\bar{p})} + 1}) = 0 = E^{off}. \end{aligned}$$

In conclusion, our online algorithm produces a solution that delivers more data than a simple offline solution using the

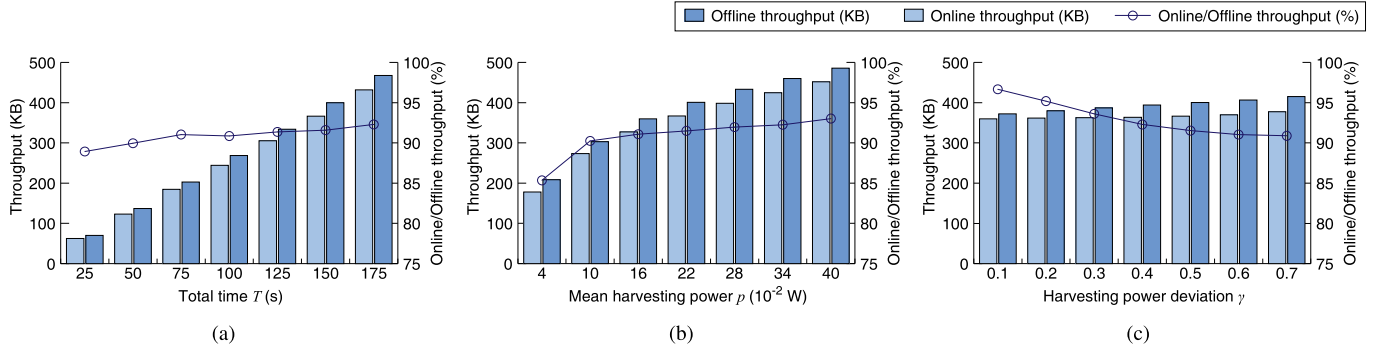


Fig. 7. The achieved throughput by the online algorithm to the offline optimal throughput. The default setting is total time $T = 150$ s, the mean harvesting power $\hat{p} = 0.22$ W, and the harvesting power deviation $\gamma = 0.5$. In (a), the total time slot T varies from 25s to 175s, with a step of 25s. In (b), the mean harvesting power \hat{p} varies from 0.04W to 0.4W with a step of 0.06W. In (c), the harvesting power deviation γ varies from 0.1 to 0.7 with a step of 0.1.

same amount of energy, *i.e.*, $B^{on} \geq B^{off}$ and $E^{on} = E^{off}$. Besides, if the harvesting power $p(t)$ is a constant and not allowed to change, *i.e.*, $\gamma = 0$, then our online algorithm generates exactly the same solution as the offline optimal solution, *i.e.*, $B^{on} = B^{off}$.

C. Simulations

In this subsection, the proposed `dam_guided_online` algorithm is implemented and its efficiency is investigated through simulations. In this evaluation, we compare the performance of the proposed online algorithm against the optimal offline solution. We also compare the performance of the proposed algorithm against the time-sharing algorithm. Note that the throughput of the optimal offline solution is the upper bound any online algorithm can ever achieve. A desired online solution is very close to the optimal offline solution.

In simulations, we assume there exists some small time interval length, in which the harvesting power does not change. We call such a small time interval a time slot. A total of T time slots are considered in evaluating the proposed algorithm, by default $T = 150$ s. For all time slots, the harvesting power is assumed to be a random variable following the uniform distribution $U((1 - \gamma)\hat{p}, (1 + \gamma)\hat{p})$, with the default mean harvesting power $\hat{p} = 0.22$ W, and default harvesting power deviation $\gamma = 0.5$.

In this simulation, we change the total time slot T , the mean harvesting power \hat{p} , and the harvesting power deviation γ , one at a time, to evaluate their impact on the algorithm performance, as in [27]. Each value shown in the figures of this section is the mean value of simulation results from 20 random instances, and in each instance, a total of T harvesting powers are generated according to the above model.

The ratio that the online algorithm achieves the offline maximum throughput is illustrated in Fig. 7, where the throughput of our online algorithm is compared to the offline optimal solution that maximizes the throughput.

In Fig. 7(a), the total time slot T varies from 25s to 175s, with a step of 25s. We can see that as the total time T increase, the throughput increases as well. Meanwhile, the larger the total time slots, the better our online algorithm performance. This is because the heart of our online algorithm is to accurately anticipate future powers, and we use the

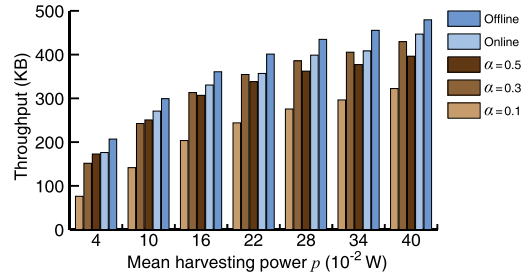


Fig. 8. The achieved throughput by the time-sharing algorithm ($\alpha = 0.1$, $\alpha = 0.3$, $\alpha = 0.5$), proposed online algorithm and proposed offline algorithm. The default setting is total time $T = 150$ s and the harvesting power deviation $\gamma = 0.5$. The mean harvesting power \hat{p} varies from 0.04W to 0.4W with a step of 0.06W.

history average harvesting power. For more time slots, the more accurate the history average is in prediction. However, even if the total time slot is only 25s, the achieved ratio is nearly 88%, and for larger total time, the achieved ratio is around 92%.

In Fig. 7(b), the mean harvesting power \hat{p} varies from 0.04W to 0.4W with a step of 0.06W. We can see that both the throughput and the efficiency of the proposed algorithm increase as the mean harvesting power \hat{p} increases. This is because when \hat{p} goes smaller, more time is needed to harvest the same amount of energy. As a result, more difficulty should be faced for our heuristic algorithm to achieve a good throughput, so its efficiency drops. However, in all tested cases, the achieved ratio stays higher than 85%.

In Fig. 7(c), the harvesting power deviation γ varies from 0.1 to 0.7 with a step of 0.1. The throughput of our online algorithm stays approximately the same while the offline algorithm increases as the deviation γ increases. This is because the larger the deviation, the more difficult it is to predict the further harvesting power. Therefore, our method based on the historical average becomes less efficient. However, we can see from the figure that even if the deviation is as high as 0.7, our online algorithm can achieve around 90% ratio.

The comparison of the proposed online and offline algorithm between time-sharing algorithm is illustrated in Fig. 8, where the mean harvesting power \hat{p} varies from 0.04W

to 0.4W with a step of 0.06W. The time-sharing algorithm is borrowed from [28], which simply divides each time slot into the harvesting period and sending period. The ratio of harvesting period to time slot is α . We here compared the throughput of the time-sharing algorithm and the optimal online and offline algorithm we proposed. We can see from the figure that in every situation, our algorithm achieved higher throughput than the time-sharing algorithm.

As a conclusion of the simulation, the proposed online algorithm is efficient and achieves more than 90% of the offline maximum throughput in most tested cases. Both the online algorithm and offline algorithm overcome the time-sharing algorithm.

VII. CONCLUSION AND FUTURE WORKS

In this paper, we first formulated the throughput maximization *HTT-scheduling* problem for the time-varying RF energy harvesting systems. Then the *wopt* power was introduced, which is with a basic but important property. Based on this property, we introduced the concept of the *dam height*. We then investigated a special case of the problem, e.g., the harvesting power is monotonically decreasing. Some optimality properties were observed, and the *dam raising system* was designed to solve the special case problem. These properties and the *dam raising system* were then extended to the general scenario, where the harvesting power can change dynamically. Finally, an online heuristic algorithm was proposed and simulations were conducted to evaluate its efficiency.

Our future work will focus on extending the system model and optimization framework to scenarios involving multiple wireless transmitters and receivers. This direction will address interference and distributed resource allocation in networked environments, thereby broadening the applicability of our results to more realistic deployment conditions.

APPENDIX

A. Proof of Theorem 4

First, we prove that the algorithm can compute the optimal HTT schedule of decreasing harvesting power. From Lemma 2 we could know that as dam height increases, the throughput monotonically increases and the remaining energy monotonically decreases. Thus, the HTT schedule of decreasing harvesting power is monotonic. Since monotonic problems can definitely be solved using bisection method, the algorithm can give optimal HTT schedule of decreasing harvesting power.

Next, we prove that the algorithm has a time complexity of $O(T \cdot \log(\frac{\rho_{max}}{\Delta}))$. When the algorithm returns at Line 11, we must have $w_{upper} - w_{lower} < \Delta$. We know that after each iteration, the value $w_{upper} - w_{lower}$ is reduced to its half. Therefore, after n iterations, we have $w_{upper} - w_{lower} = \frac{1}{2^n}w_{max}$. Therefore, when the algorithm returns at Line 11, we have $\frac{1}{2^n}w_{max} < \Delta$, which could be equivalently written as $n > \log_2(\frac{w_{max}}{\Delta})$. Note that in each iteration, we invoke *is_shortage* for $O(T)$ times. So, the overall time complexity is $O(T \cdot \log(\frac{\rho_{max}}{\Delta}))$.

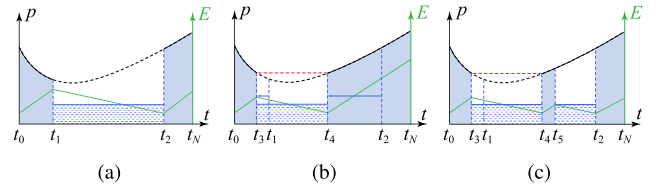


Fig. 9. The process of improving the throughput of the “left low, right high” situation.

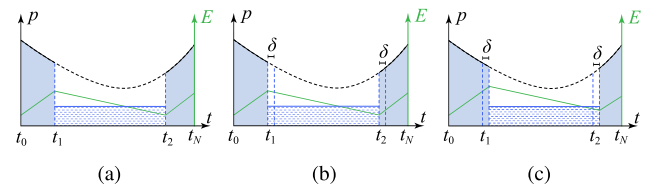


Fig. 10. The process of improving the throughput of the “left high, right low” situation.

B. Proof of Theorem 5

We prove this theorem by contradiction. In the optimal schedule, assume, for contradictory, there does not exist time τ_i and power level w_i for interval $[\tau_{i-1}, \tau_i]$ such that in the interval any charging phase has $p(t) > w_i$ and any sending phase has $p(t) \leq w_i$, then, we claim there is at least one sending phase has different $p(t)$ on its both ends. The core idea of our method is to show such a schedule can be further improved, contradicting to its optimality assumption.

There are only two situations where the $p(t)$ on both ends of the sending phase are not equal: the right end is higher, or the left end is higher. Let’s call the situation where the right end is higher the “left low, right high” and the situation where the left end is higher the “left high, right low”, which are shown in Fig. 9 and 10.

We first consider the “left low, right high” situation, which is shown in Fig. 9(a). Suppose the sending phase is $t_1 \sim t_2$ and $p(t_1) < p(t_2)$ and the sending power is ρ . Suppose $E(t_2) = C$, where C is a constant and $C \geq 0$. Therefore, we have:

$$E(t_0) + \int_{t_0}^{t_1} p(t) dt - \rho(t_2 - t_1) = C. \quad (17)$$

The first step is to move t_1 and t_2 forward, which is shown in Fig. 9(b). We move t_1 and t_2 forward to t_3 and t_4 . In this process we keep $E(t_4) = C$, until we find a pair of (t_3, t_4) such that $p(t_3) = p(t_4)$. We could always find (t_3, t_4) , unless t_3 touches the start point, which turned out to be a fast-switching cycle. Note that the sending power is still ρ here. Because $t_1 = t_3 + (t_1 - t_3)$, Eq. (17) could also be written as

$$E(t_0) + \int_{t_0}^{t_3} p(t) dt + \int_{t_3}^{t_1} p(t) dt - \rho(t_2 - t_1) = C. \quad (18)$$

The second step is to find t_5 , which is shown in Fig. 9(c). We need to find t_5 between t_4 and t_2 such that $E(t_N)$ remains the same because $E(t_N)$ is different between Fig. 9(a) and Fig. 9(b). Therefore, we have:

$$\begin{aligned} E(t_0) + \int_{t_0}^{t_3} p(t) dt + \int_{t_4}^{t_5} p(t) dt \\ - \rho(t_4 - t_3) - \rho(t_2 - t_5) = C. \end{aligned} \quad (19)$$

Subtract Eq. (18) from Eq. (19) and we have:

$$\int_{t_4}^{t_5} p(t) dt - \int_{t_3}^{t_1} p(t) dt = \rho(t_1 - t_3) - \rho(t_5 - t_4). \quad (20)$$

We claim that $t_5 - t_4$ must no greater than $t_1 - t_3$. Otherwise, we will find that, comparing Fig. 9(a) with Fig. 9(c), more energy is charged and less energy is used, however, the remaining energy stays the same, which is a contradiction. The details of the proof are as follows:

Suppose $t_5 - t_4 > t_1 - t_3$. Add t_2 on both sides so

$$t_2 + t_5 - t_4 > t_2 + t_1 - t_3.$$

Move $t_5 - t_4$ and t_1 to opposite side, and we have

$$t_2 - t_1 > t_2 - t_5 + t_4 - t_3.$$

The left part of the inequality is the length of the sending phase in Fig. 9(a) and the right part is the length of sending phases in Fig. 9(c). Note that the sending power is always ρ . Therefore, the energy used to send in Fig. 9(a) is larger than that in Fig. 9(c).

Meanwhile, from Fig. 9(c) we could find that $p(t)$ is larger in $t_4 \sim t_5$ than that in $t_3 \sim t_1$. Note that $t_5 - t_4$ is also greater than $t_1 - t_3$. Therefore, we have

$$\int_{t_4}^{t_5} p(t) dt > \int_{t_3}^{t_1} p(t) dt$$

Add $\int_{t_0}^{t_3} p(t) dt$ on both sides, and we get:

$$\int_{t_0}^{t_3} p(t) dt + \int_{t_4}^{t_5} p(t) dt > \int_{t_0}^{t_3} p(t) dt + \int_{t_3}^{t_1} p(t) dt$$

which could be also written as

$$\int_{t_0}^{t_3} p(t) dt + \int_{t_4}^{t_5} p(t) dt > \int_{t_0}^{t_1} p(t) dt.$$

The right part of the inequality is the harvested energy in Fig. 9(a) and the left part is the harvested energy in Fig. 9(c). Therefore, the energy harvested in Fig. 9(a) is less than that in Fig. 9(c). Therefore, the relationship of harvested energy between Fig. 9(a) and Fig. 9(c) contradicts the relationship of sending-used energy between Fig. 9(a) and Fig. 9(c). Therefore, $t_5 - t_4$ must no greater than $t_1 - t_3$.

Add t_2 on both sides of $t_5 - t_4 \leq t_1 - t_3$, and we have

$$t_2 + t_5 - t_4 \leq t_2 + t_1 - t_3.$$

Move $t_5 - t_4$ and t_1 to opposite side, and we have

$$t_2 - t_1 \leq t_2 - t_5 + t_4 - t_3.$$

The left part of the inequality is the length of the sending phase in Fig. 9(a) and the right part is the length of the sending phases in Fig. 9(c). Note that the sending power is always ρ . Therefore, the sending rate is always a constant, which is $\log(1 + \rho)$. Therefore, the throughput in Fig. 9(c) is no less than that in Fig. 9(a). Therefore, we improved the throughput of the “left low, right high” situation.

Next, we consider the “left high, right low” situation, which is shown in Fig. 10(a). Suppose the sending phase is $t_1 \sim t_2$, $p(t_1) > p(t_2)$, and sending power is ρ . We continuously perform the following operations until $p(t_1) = p(t_2)$.

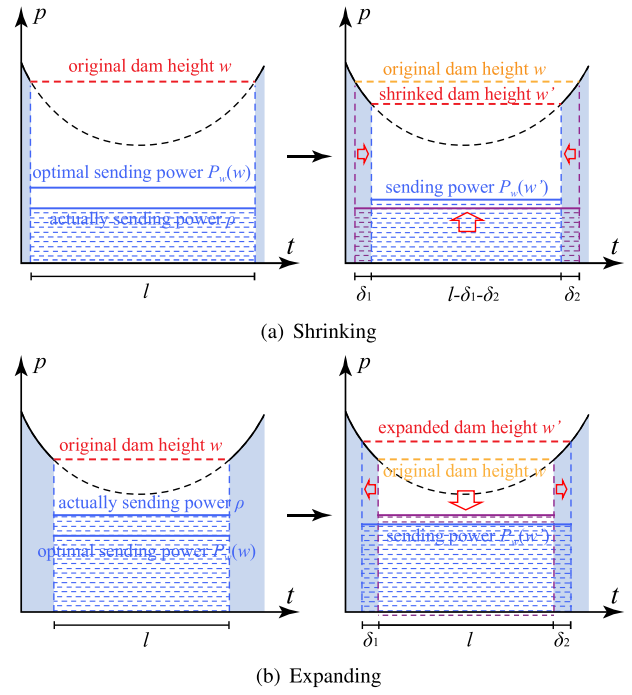


Fig. 11. If actually sending power ρ is smaller (larger) than the optimal sending power $P_w(w)$, we can expand (shrink) the sending phase to improve the solution.

First, we select a short interval of δ after t_1 and t_2 , which is shown in Fig. 10(b). δ must satisfy the following condition: every $p(t)$ in $t_1 \sim t_1 + \delta$ must be greater than that in $t_2 \sim t_2 + \delta$. Therefore, we have:

$$\int_{t_1}^{t_1+\delta} p(t) dt > \int_{t_2}^{t_2+\delta} p(t) dt.$$

That is to say, the harvested energy in $t_1 \sim t_1 + \delta$ is larger than that in $t_2 \sim t_2 + \delta$. Then we swap these two intervals, which is shown in Fig. 10(c). Swapping is always feasible. Because by swapping, we first harvest and then send. After swapping, the remaining energy at $t_2 + \delta$ should be larger than 0 because the harvested energy in $t_1 \sim t_1 + \delta$ is larger than that in $t_2 \sim t_2 + \delta$. The excess remaining energy could be used to increase sending power in the sending phase. Therefore, the throughput could be improved.

By continuously perform these operations, $p(t_1)$ will eventually equal to $p(t_2)$. Therefore, we improved the throughput of the “left high, right low” situation.

Therefore, the $p(t)$ on both ends of the sending phase should be the same, otherwise, we can always improve.

C. Proof of Lemma 3

Here we draw Fig. 11 to show how we expand and shrink. Below we prove the existence of the operation.

We first consider the situation of shrinking, which is shown in Fig. 11(a). Suppose the original dam height is w . Therefore, according to Eq. (8), the optimal sending power is $P_w(w)$. Suppose the actually sending power is ρ , and $P_w(w) > \rho$.

Assume we exclude a small duration of δ_1 at the beginning and exclude δ_2 at the end. Note that after we shrink, both ends are still at the same height w' . Here we use E_1 to represent

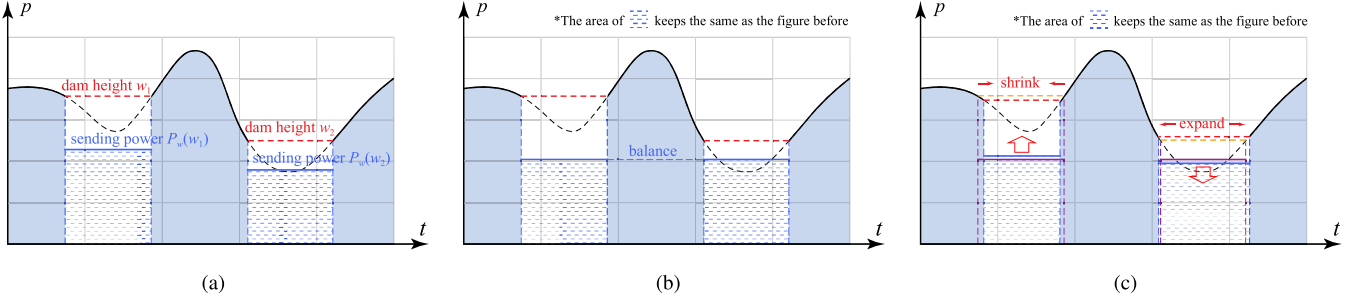


Fig. 12. The process of improving throughput while not increasing energy consumption. (a) A common situation where has two different dam heights. (b) The balance operation. (c) The shrinking and expanding operation.

the energy consumed in the sending period before we shrink and E_2 represents that after we shrink. Therefore, we have

$$\begin{aligned} E_1 &= -\rho l \\ E_2 &= \int_{\delta_1} p(t) dt + \int_{\delta_2} p(t) dt - (l - \delta_1 - \delta_2) P_w(w') \end{aligned}$$

Assume ΔE is the difference of energy consumption between the schedules before and after we shrink. Therefore, we have:

$$\begin{aligned} \Delta E &= E_2 - E_1 \\ &= \int_{\delta_1} p(t) dt + \int_{\delta_2} p(t) dt \\ &\quad + (l\rho - (l - \delta_1 - \delta_2) P_w(w')). \end{aligned}$$

When $\delta_1 + \delta_2 = l$, we have:

$$\Delta E = \int_{\delta_1} p(t) dt + \int_{\delta_2} p(t) dt + \rho l > 0.$$

When $\delta_1 + \delta_2 = 0$, which means $w = w'$, we have:

$$\Delta E = l(\rho - P_w(w')) = l(\rho - P_w(w)) < 0.$$

Note that ΔE is a continuous function of δ_1 and δ_2 . Therefore, according to Bolzano's Theorem there exists a pair of (δ_1, δ_2) which let $\Delta E = 0$. Therefore, there exists an operation that meets the first constraint.

Next, we prove this operation meets the second constraint, which means the operation doesn't decrease the throughput. Compared with the case before we shrink, the harvested energy that can be used in sending is $\int_{\delta_1} p(t) dt + \int_{\delta_2} p(t) dt$ more. Let $\delta = \delta_1 + \delta_2$ and $\rho' = P_w(w')$. Note that

$$\int_{\delta_1} p(t) dt + \int_{\delta_2} p(t) dt > w'(\delta_1 + \delta_2) = w'\delta.$$

Let's ignore the difference between $\int_{\delta_1} p(t) dt + \int_{\delta_2} p(t) dt$ and $w'\delta$, because if we don't decrease throughput with less energy, we won't decrease the throughput with more energy.

Suppose we used E energy before we shrink. We have $E + w'l = \rho l + w'l$, hence $l = \frac{E+w'l}{w'+\rho}$, and therefore

$$B = (E + w'l) \frac{\log(1 + \rho)}{w' + \rho}. \quad (21)$$

After we shrink, we have

$$\rho'(l - \delta) = E + w'\delta.$$

We have $(w' + \rho')(l - \delta) = E + w'\delta - w'\delta + w'l$, hence $l - \delta = \frac{E+w'l}{w'+\rho'}$, and therefore

$$B' = (E + w'l) \frac{\log(1 + \rho')}{w' + \rho'}. \quad (22)$$

By treating ρ as a variable, the throughput is a function of ρ . Through the analysis of Eq. (7) and the Fig. 3, we can easily conclude that when $P_w(w') > \rho' \geq \rho$, we have $B' \geq B$. Therefore, this operation meets the second constraint.

The proof of expanding is the same as shrinking, which will not be further elaborated here.

D. Proof of Theorem 6

We will use Lemma 3 (Expanding and shrinking) to prove Theorem 6 here. Suppose there is a sending phase in the optimal HTT schedule where sending power ρ is not $P_w(w)$. w is the dam height of the sending phase. According to Lemma 3, the shrinking(expanding) doesn't change the energy consumption. Moreover, the shrinking(expanding) will not decrease the throughput. Therefore, we could apply shrinking(expanding) on the sending phase. And the throughput after we apply shrinking(expanding) will be no less than that before. Therefore, we improved the optimal HTT schedule, which is a contradiction. Therefore, in each sending phase of the optimal HTT schedule, the sending power should be $P_w(w)$, where w is the dam height of the sending phase.

E. Proof of Lemma 4

Consider a common situation shown in the Fig. 12(a). Assume there are two sending phases. The dam heights and sending power of these two sending phases are w_1, w_2 and $P_w(w_1), P_w(w_2)$. Note that $w_1 \neq w_2$. By performing the following operations, we could improve the throughput without increasing energy consumption.

First we balance the sending power of two sending phases, which is shown in Fig. 12(b). Suppose the lengths of two sending phases are l_1 and l_2 . For the sake of convenience in our proof, let $\rho_1 = P_w(w_1)$, $\rho_2 = P_w(w_2)$ and denote ρ_3 as the balanced sending power. The premise of the balance operation is not to increase energy consumption, which means the areas of sending phases are equal in Fig. 12(a) and Fig. 12(b). Thus,

$$\rho_1 l_1 + \rho_2 l_2 = \rho_3 (l_1 + l_2).$$

Therefore,

$$\rho_3 = \frac{\rho_1 l_1 + \rho_2 l_2}{l_1 + l_2}. \quad (23)$$

Before we perform the balance operation, the throughput is $l_1 \log(1 + \rho_1) + l_2 \log(1 + \rho_2)$. After we perform the operation, the throughput is $(l_1 + l_2) \log(1 + \rho_3)$. Because the concavity of the power-rate function, we could use the Jensen's inequality. Thus, we have

$$\frac{l_1 \log(1 + \rho_1) + l_2 \log(1 + \rho_2)}{l_1 + l_2} < \log\left(1 + \frac{\rho_1 l_1 + \rho_2 l_2}{l_1 + l_2}\right). \quad (24)$$

By substituting Eq. (23) into Eq. (24), we can get

$$l_1 \log(1 + \rho_1) + l_2 \log(1 + \rho_2) < (l_1 + l_2) \log(1 + \rho_3). \quad (25)$$

Note that the left part of Eq. (25) is the throughput before the operation and the right part is the throughput after the operation. Therefore, the balance operation improves the throughput without increasing energy consumption.

Next, we perform shrinking and expanding operations in two sending phases. According to the Lemma 3, both the shrinking and expanding operations do not increase the energy consumption and both the operations do not decrease the throughput. Therefore, the throughput is improved without increasing energy consumption after we perform these two operations in the sending phases.

Note that after performing operations shown in Fig. 12(b) and Fig. 12(c), the difference between w_1 and w_2 decreased. This is because the shrinking(expanding) operation shortened the length of the left(right) sending phase. Therefore, the dam height of the left(right) sending phase in Fig. 12(c) decreased(increased) compared with Fig. 12(a). Thus, the difference between w_1 and w_2 decreased.

By continuously performing operations in Fig. 12(b) and Fig. 12(c), the dam heights of the two sending phases will eventually reach the same height. In this process, the throughput was improved while the energy consumption was not increased.

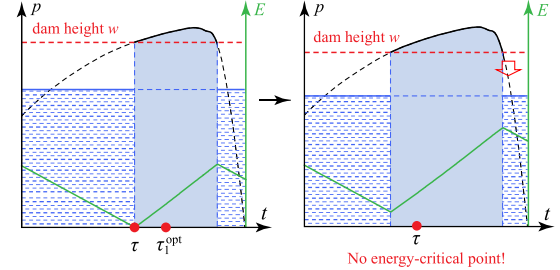
F. An Example of the Optimal Solution

An example of the optimal solution that satisfy Lemma 5, 6, and Definition 6 is given in Fig. 14.

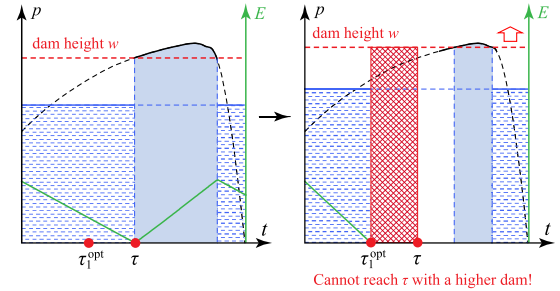
G. Proof of Theorem 7

First, we prove that the algorithm can compute the optimal HTT schedule for the offline problem. In every iteration of the **while** loop, the same problem repeats, that is starting from τ_0 , find the next optimal changing point and the corresponding dam height. We, therefore, need only to show that in the first iteration, where $\tau_0 = 0$, the dam height w and changing time τ are optimally set in Line 5, i.e., $\tau_1^{opt} = \tau$ and $w_1^{opt} = w$. Here we prove it by employing proof by contradiction.

Suppose, on the contrary, the first optimal changing point $\tau_1^{opt} \neq \tau$, where τ is returned by `find_emptyP`. We then have the following two cases: (1) $\tau_1^{opt} > \tau$ and (2) $\tau_1^{opt} < \tau$.



(a) $\tau_1^{opt} > \tau$. After we lowered the dam, we couldn't find any energy-critical point. This contradicts τ_1^{opt} .



(b) $\tau_1^{opt} < \tau$. After raising the dam, we need to reach τ with a higher dam height according to Lemma 5. However, this is impossible.

Fig. 13. If $\tau_1^{opt} \neq \tau$, then there are two cases: $\tau_1^{opt} > \tau$ and $\tau_1^{opt} < \tau$.

Case $\tau_1^{opt} > \tau$, illustrated in Fig. 13(a). We must have $w_1^{opt} < w$ because the dam height w already makes the battery energy-critical at τ , we have to lower the dam to make the energy-critical at τ_1^{opt} . Since w returned by `dam_raising_shotg` is the highest feasible dam height position w and the battery is energy-critical at time τ for the first time, then, for dam height lower than w , there doesn't exist energy-critical point. Then, it is impossible to have a single dam height that can make the battery energy-critical at any time $t > \tau$.

Case $\tau_1^{opt} < \tau$, illustrated in Fig. 13(b). We must have $w_1^{opt} > w$ because the dam height w does not make the battery energy-critical at any time $t < \tau$, we have to raise the dam to make the energy-critical at τ_1^{opt} . We claim that in the optimal dam heights, there is at least one dam height w_i^{opt} in (or partially in) duration $[\tau_1^{opt}, \tau]$, such that $w_i^{opt} < w$. Otherwise, optimal dam heights in $[0, \tau]$ are all greater than w , contradicting the fact that w depletes battery at τ . This is a contradiction to Lemma 5.

Therefore, the first optimal changing point $\tau_1^{opt} = \tau$. In this way, the size of the problem becomes smaller. By using the proof again, we can show that the algorithm can compute the optimal HTT schedule for the offline problem.

Next, we prove that the algorithm has a time complexity of $O(T^2 \log(\frac{\rho_{max}}{\Delta}) / \Delta t)$. From Theorem 4 we could know that the algorithm `dam_raising_shotg` has a time complexity of $O(T \cdot \log(\frac{\rho_{max}}{\Delta}))$. In every **while** loop, we at least let τ_0 increase Δt . Because the worst situation is that we couldn't raise the dam, therefore, $\tau = \tau_0$. In the worst situation we assign $\tau + \Delta t$ to τ_0 , that is, let τ_0 increase Δt . Therefore, in every **while** loop, we at least let τ_0 increase Δt . As a result, the **while** loop will at most run $T/\Delta t$ times. In every **while** loop, we will run `dam_raising_shotg`

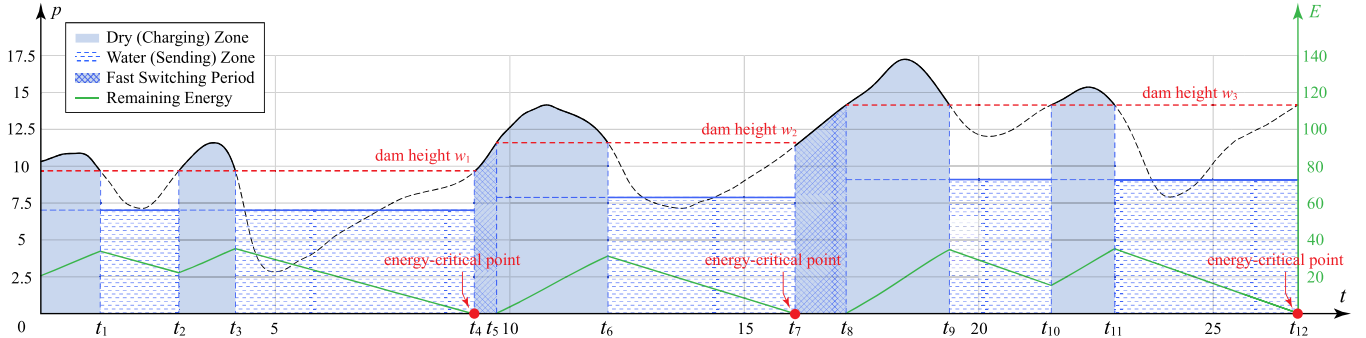


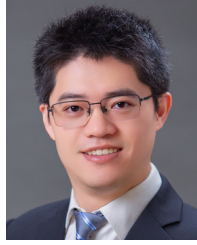
Fig. 14. An example of the optimal solution for the general harvesting power $p(t)$.

once and its time complexity is $O(T \cdot \log(\frac{\rho_{max}}{\Delta}))$. We also run `find_emptyP` once and its time complexity is $O(T)$. Therefore, the time complexity of each **while** loop is $\max(O(T \cdot \log(\frac{\rho_{max}}{\Delta})), O(T)) = O(T \cdot \log(\frac{\rho_{max}}{\Delta}))$. Note that we just proved that the **while** loop will at most run $T/\Delta t$ times. Therefore, the algorithm has a time complexity of $O(T/\Delta t \cdot T \cdot \log(\frac{\rho_{max}}{\Delta})) = O(T^2 \log(\frac{\rho_{max}}{\Delta})/\Delta t)$.

REFERENCES

- [1] J. Li et al., "MagFingerprint: A magnetic based device fingerprinting in wireless charging," in *Proc. IEEE Conf. Comput. Commun.*, May 2023, pp. 1–10.
- [2] W. Zhou, H. Zhou, X. Cui, X. Wang, X. Wang, and Z. Liu, "Roland: Robust in-band parallel communication for magnetic MIMO wireless power transfer system," in *Proc. IEEE Conf. Comput. Commun.*, May 2023, pp. 1–10.
- [3] M. Ren, D. Wu, J. Xue, W. Xu, J. Peng, and T. Liu, "Utilizing the neglected back lobe for mobile charging," in *Proc. IEEE Conf. Comput. Commun.*, May 2023, pp. 1–10.
- [4] Y. Ma, D. Wu, M. Ren, J. Peng, J. Yang, and T. Liu, "Concurrent charging with wave interference," in *Proc. IEEE Conf. Comput. Commun.*, May 2023, pp. 1–10.
- [5] P. Zhou, C. Wang, and Y. Yang, "Design and optimization of electric autonomous vehicles with renewable energy source for smart cities," in *Proc. IEEE Conf. Comput. Commun.*, Jul. 2020, pp. 1399–1408.
- [6] R. Guida, E. Demirors, N. Dave, and T. Melodia, "Underwater ultrasonic wireless power transfer: A battery-less platform for the Internet of Underwater Things," *IEEE Trans. Mobile Comput.*, early access, Oct. 8, 2022, doi: [10.1109/TMC.2020.3029679](https://doi.org/10.1109/TMC.2020.3029679).
- [7] V. Liu, A. Parks, V. Talla, S. Gollakota, D. Wetherall, and J. R. Smith, "Ambient backscatter: Wireless communication out of thin air," in *Proc. ACM SIGCOMM Conf. SIGCOMM*, Aug. 2013, pp. 39–50.
- [8] S. Mohanti, E. Bozkaya, M. Y. Naderi, B. Canberk, G. Secinti, and K. R. Chowdhury, "WiFED mobile: WiFi friendly energy delivery with mobile distributed beamforming," *IEEE/ACM Trans. Netw.*, vol. 29, no. 3, pp. 1362–1375, Jun. 2021.
- [9] V. Iyer, V. Talla, B. Kellogg, S. Gollakota, and J. Smith, "Inter-technology backscatter: Towards Internet connectivity for implanted devices," in *Proc. Annu. Conf. ACM Special Interest Group Data Commun. Appl., Technol., Architectures, Protocols Comput. Commun. (SIGCOMM)*, Aug. 2016, pp. 1–14.
- [10] (2023). About Powercast. [Online]. Available: <https://www.powercastco.com>
- [11] (2023). Wireless Identification and Sensing Platform (WISP). [Online]. Available: <https://sites.google.com/uw.edu/wisp-wiki/home>
- [12] S. Li, S. He, K. Hu, L. Fu, S. Chen, and J. Chen, "Operation state scheduling towards optimal network utility in RF-powered Internet of Things," *IEEE Trans. Mobile Comput.*, early access, May 18, 2021, doi: [10.1109/TMC.2020.2995256](https://doi.org/10.1109/TMC.2020.2995256).
- [13] K.-G. Nguyen, Q.-D. Vu, L.-N. Tran, and M. Junutti, "Energy efficiency fairness for multi-pair wireless-powered relaying systems," *IEEE J. Sel. Areas Commun.*, vol. 37, no. 2, pp. 357–373, Feb. 2019.
- [14] A. H. Sakr and E. Hossain, "Analysis of K -tier uplink cellular networks with ambient RF energy harvesting," *IEEE J. Sel. Areas Commun.*, vol. 33, no. 10, pp. 2226–2238, Oct. 2015.
- [15] T. A. Zewde and M. C. Gursoy, "Optimal resource allocation for energy-harvesting communication networks under statistical QoS constraints," *IEEE J. Sel. Areas Commun.*, vol. 37, no. 2, pp. 313–326, Feb. 2019.
- [16] F. Shan, J. Luo, W. Wu, and X. Shen, "Optimal wireless power transfer scheduling for delay minimization," in *Proc. 35th Annu. IEEE Int. Conf. Comput. Commun.*, Apr. 2016, pp. 1–9.
- [17] F. Shan, J. Luo, W. Wu, and X. Shen, "Delay minimization for data transmission in wireless power transfer systems," *IEEE J. Sel. Areas Commun.*, vol. 37, no. 2, pp. 298–312, Feb. 2019, doi: [10.1109/JSAC.2018.2872395](https://doi.org/10.1109/JSAC.2018.2872395).
- [18] M. A. Qureshi and C. Tekin, "Online Bayesian learning for rate selection in millimeter wave cognitive radio networks," in *Proc. IEEE Conf. Comput. Commun.*, Jul. 2020, pp. 1449–1458.
- [19] H. Ju and R. Zhang, "Throughput maximization in wireless powered communication networks," *IEEE Trans. Wireless Commun.*, vol. 13, no. 1, pp. 418–428, Jan. 2014.
- [20] F. Zhao, L. Wei, and H. Chen, "Optimal time allocation for wireless information and power transfer in wireless powered communication systems," *IEEE Trans. Veh. Technol.*, vol. 65, no. 3, pp. 1830–1835, Mar. 2016.
- [21] X. Song and K.-W. Chin, "Maximizing packets collection in wireless powered IoT networks with charge-or-data time slots," *IEEE Trans. Cognit. Commun. Netw.*, vol. 9, no. 4, pp. 106–1079, Aug. 2023.
- [22] C. Jin, F. Hu, Z. Ling, Z. Mao, Z. Chang, and C. Li, "Transmission optimization and resource allocation for wireless powered dense vehicle area network with energy recycling," *IEEE Trans. Veh. Technol.*, vol. 71, no. 11, pp. 12291–12303, Nov. 2022.
- [23] H. Kim, T. Cho, J. Lee, W. Shin, and H. Vincent Poor, "Optimized shallow neural networks for sum-rate maximization in energy harvesting downlink multiuser NOMA systems," *IEEE J. Sel. Areas Commun.*, vol. 39, no. 4, pp. 982–997, Apr. 2021.
- [24] M. Zhang, J. Huang, and R. Zhang, "Wireless power transfer with information asymmetry: A public goods perspective," *IEEE Trans. Mobile Comput.*, vol. 20, no. 1, pp. 276–291, Jan. 2021.
- [25] R. M. Corless, G. H. Gonnet, D. E. G. Hare, D. J. Jeffrey, and D. E. Knuth, "On the Lambert W function," *Adv. Comput. Math.*, vol. 5, p. 329, Sep. 1996.
- [26] J. Yang and S. Ulukus, "Optimal packet scheduling in an energy harvesting communication system," *IEEE Trans. Commun.*, vol. 60, no. 1, pp. 220–230, Jan. 2012.
- [27] B. Wang, X. Yang, G. Wang, G. Yu, W. Zang, and M. Yu, "Energy efficient approximate self-adaptive data collection in wireless sensor networks," *Frontiers Comput. Sci.*, vol. 10, no. 5, pp. 936–950, Oct. 2016.
- [28] B. Clerckx, J. Kim, K. W. Choi, and D. I. Kim, "Foundations of wireless information and power transfer: Theory, prototypes, and experiments," *Proc. IEEE*, vol. 110, no. 1, pp. 8–30, Jan. 2022.
- [29] S. Shen, J. Kim, C. Song, and B. Clerckx, "Wireless power transfer with distributed antennas: System design, prototype, and experiments," *IEEE Trans. Ind. Electron.*, vol. 68, no. 11, pp. 10868–10878, Nov. 2021.
- [30] O. L. A. López et al., "Energy-sustainable IoT connectivity: Vision, technological enablers, challenges, and future directions," *IEEE Open J. Commun. Soc.*, vol. 4, pp. 2609–2666, 2023.

- [31] O. L. A. López, E. M. G. Fernández, R. D. Souza, and H. Alves, "Wireless powered communications with finite battery and finite blocklength," *IEEE Trans. Commun.*, vol. 66, no. 4, pp. 1803–1816, Apr. 2018.
- [32] R. Valentini, M. Levorato, and F. Santucci, "Optimal aging-aware channel access and power allocation for battery-powered devices with radio frequency energy harvesting," *IEEE Trans. Commun.*, vol. 66, no. 11, pp. 5773–5787, Nov. 2018.
- [33] L. Huang et al., "Throughput guarantees for multi-cell wireless powered communication networks with non-orthogonal multiple access," *IEEE Trans. Veh. Technol.*, vol. 71, no. 11, pp. 12104–12116, Nov. 2022.
- [34] H.-H. Choi, W. Shin, M. Levorato, and H. V. Poor, "Harvest-or-access: Slotted ALOHA for wireless powered communication networks," *IEEE Trans. Veh. Technol.*, vol. 68, no. 11, pp. 11394–11398, Nov. 2019.
- [35] G. Karadag, M. S. Iqbal, and S. Coleri, "Optimal power control, scheduling, and energy harvesting for wireless networked control systems," *IEEE Trans. Commun.*, vol. 69, no. 3, pp. 1789–1801, Mar. 2021.
- [36] F. Shan et al. *Optimal Harvest-then-Transmit Scheduling for Throughput Maximization in Time-varying RF Powered Systems (Extended Version)*. Accessed: Sep. 18, 2024. [Online]. Available: <https://fengshan.seunetsi.net/papers/SLJCWLDSAC24-extended.pdf>



Feng Shan (Member, IEEE) received the Ph.D. degree in computer science from Southeast University, Nanjing, China, in 2015. He was a Visiting Student with the School of Computing and Engineering, University of Missouri-Kansas City, Kansas City, MO, USA, from 2010 to 2012. He is currently an Associate Professor with the School of Computer Science and Engineering, Southeast University. His research interests include the Internet of Things, wireless networks, swarm intelligence, and algorithm design and analysis.



SMC Technical Committee on Computer Supported Cooperative Work in Design and the ACM China Awards Committee.

Junzhou Luo (Senior Member, IEEE) received the B.Sc. degree in applied mathematics and the M.S. and Ph.D. degrees in computer network from Southeast University, China, in 1982, 1992, and 2000, respectively. He is currently a Full Professor with the School of Computer Science and Engineering, Southeast University. His research interests include network architecture, network security, cloud computing, wireless networks, and the Internet of Things. He is a member of the IEEE Computer Society and ACM. He is the Co-Chair of the IEEE



Liwen Cao is currently pursuing the B.Sc. degree with the School of Computer Science and Engineering, Southeast University, Nanjing, China. His research interests include computer vision and optimization algorithms.



Weiwei Wu (Member, IEEE) received the B.Sc. degree in computer science from the South China University of Technology (SCUT) in 2006 and the joint Ph.D. degree in computer science from the City University of Hong Kong (CityU) and the University of Science and Technology of China (USTC) in 2011. He went to the Mathematical Division, Nanyang Technological University (NTU), Singapore, for post-doctoral research, in 2012. He is currently a Professor with the School of Computer Science and Engineering, Southeast University, China. His research interests include optimizations and algorithm analysis, crowdsourcing, reinforcement learning, game theory, wireless communications, and network economics.



Zhen Ling (Member, IEEE) received the B.S. degree from Nanjing Institute of Technology, Nanjing, China, in 2005, and the Ph.D. degree in computer science from Southeast University, Nanjing, in 2014. He is currently a Professor with the School of Computer Science and Engineering, Southeast University. His research interests include network security, privacy, and the Internet of Things. He received the ACM China Doctoral Dissertation Award in 2014 and China Computer Federation Doctoral Dissertation Award in 2015.



Qiao Jin is currently pursuing the B.Sc. degree with the School of Computer Science and Engineering, Southeast University, Nanjing, China. His research interests include algorithm design and high performance computing.



Fang Dong (Member, IEEE) received the Ph.D. degree in computer science from Southeast University, China, in 2011. He is currently a Full Professor with the School of Computer Science and Engineering, Southeast University. His current research interests include edge intelligence, cloud computing, and industrial internet. He is a member of ACM. He served as the Co-Chair for the ACM Nanjing Chapter.